Articles in PresS. Am J Physiol Renal Physiol (December 9, 2015). doi:10.1152/ajprenal.00208.2015

Comparative expression of the extracellular calcium sensing receptor in mouse, rat and human kidney.

Graca JAZ[1,2], Schepelmann M[2], Brennan SC[2], Reens J[1], Chang W[3], Yan P[4], Toka H[4], Riccardi D[2*] and Price SA[1*]

*SAP and DR contributed equally to this work

[1]Pathology Sciences, AstraZeneca R&D, Mereside, Alderley Park, Macclesfield, Cheshire, SK10 4TG, UK

[2]School of Biosciences, Cardiff University, The Sir Martin Evans Building, Museum Avenue, Cardiff, CF10 3AX, UK

[3]Department of Medicine, UCSF School of Medicine, San Francisco, CA 94143, USA

[4]Division of Nephrology, Beth Israel Deaconess Medical Center, 99 Brookline Ave, RN320 Boston, MA 02215, USA

[5]Division of Nephrology and Hypertension, Eastern Virginia Medical School, Norfolk, VA 23510, USA

Corresponding Author:

Sally Price, PhD

BioHub at Alderley Park

Alderley Park, Macclesfield, UK

Telephone +44 (0) 1625 238814

E-mail: sally.price@biohubatalderley.co.uk

Keywords: calcium-sensing receptor, kidney, localization, proximity ligation assay, antibody

Contributions:

JAZG, MS, SCB, PY, JR performed the experiments

WC, HT contributed analytical tools

JAZG, MS, SCB, DR, SAP designed the research

JAZG, DR, SAP wrote the manuscript

Abstract

The calcium sensing receptor (CaSR) was cloned over 20 years ago and functionally demonstrated to regulate circulating levels of parathyroid hormone by maintaining physiological serum ionized calcium (Ca^{2+}) concentration. The receptor is highly expressed in the kidney; however, intra-renal and intra-species distribution remains controversial. Recently, additional functions of the CaSR receptor in the kidney have emerged, including parathyroid hormone independent effects. It is therefore critical to establish unequivocally the localization of the CaSR in the kidney in order to relate this to its proposed physiological roles. In this study we determined CaSR expression in mouse, rat and human kidney using *in situ* hybridisation, immunohistochemistry (using eight different commercially available and custom-made antibodies) and proximity ligation assays. Both in situ hybridisation and immunohistochemistry showed CaSR expression in the thick ascending limb, distal tubule and collecting duct of all species, with the thick ascending limb showing the highest levels. Within the collecting ducts there was significant heterogeneity of expression between cell types. In the proximal tubule, lower levels of immunoreactivity were detected by immunohistochemistry and proximity ligation assays. Proximity ligation assays were the only technique to demonstrate expression within glomeruli. This study demonstrated CaSR expression throughout the kidney with minimal discrepancy between species but with significant variation in the levels of expression between cell and tubule types. These findings clarify the intra-renal distribution of the CaSR and enable elucidation of the full physiological roles of the receptor within this organ.

Introduction

The calcium sensing receptor (CaSR) is a G-protein coupled receptor with a key role in extracellular free ionized calcium (Ca^{2+}_o) homeostasis. The CaSR was first cloned and characterized in the parathyroid by Brown and coworkers in 1993 (7) and subsequently identified in other organs involved in the control of Ca^{2+}_o, namely the kidney (37), GI tract (15) and bone (18). In addition, CaSR expression has been reported in tissues outside the Ca^{2+}_o homeostatic system such as the blood vessels (8), thyroid (16), nerve (38) and heart (42). In kidney the CaSR regulates calcium excretion by modulating the actions of parathyroid hormone (PTH) (26). However, the CaSR also regulates calcium excretion in a PTH-independent way, by controlling paracellular movement of Ca^{2+} in the thick ascending limb (TAL) through modulation of both the transepithelial potential difference and paracellular permeability (17, 40). Additional functions of the renal CaSR include renin release (23, 29), acidification (13, 33) and concentration of urine (39). The distribution of intra-renal CaSR is critical to elucidating the full functional role of the receptor. The initial characterization of CaSR expression in rat kidney assessed the distribution of CaSR mRNA by northern blot and *in situ* hybridization (ISH) (36, 37). Transcripts were detected predominantly in outer medulla and cortex, with stronger expression in the cortical medullary rays, indicating a predominant expression of CaSR in the TAL (37). More detailed analysis of transcripts in rat kidney using ISH and reverse transcription polymerase chain reaction (RT-PCR) in dissected rat nephron segments, demonstrated expression in glomeruli, proximal tubules (PT), medullary (mTAL) and cortical (cTAL) TAL, distal tubules (DT) and collecting ducts (CD) (36). Comparable protein distribution was subsequently described in

rat kidney using immunofluorescence; expression was observed in PT, mTAL, cTAL, macula densa cells, DT and type A intercalated cells in cortical CDs (CCDs). In addition, the authors observed different cellular polarity of the receptor in different cell types along the nephron (35). Over the last decade, more detailed studies have been undertaken to address the precise localisation of the CaSR within the glomerulus. Expression has been demonstrated in juxtaglomerular cells (23, 29), activation of which inhibits renin release via an indirect effect on enzymes (adenylyl cyclase 5, phosphodiesterase 1C) that are the targets of the classical renin stimuli (30). Furthermore, calcimimetics inhibit plasma renin activity in a PTH-independent fashion both *in vitro* and *in vivo* (1, 20, 23). Consistent with CaSR expression in glomerular podocytes, calcimimetics ameliorate toxin-induced glomerulosclerosis via antiapoptotic and cytoskeleton-stabilizing effects (28). CaSR expression has also been demonstrated in mouse (20) and human (25) mesangial cells and has been shown to mediate Ca^{2+} influx and cell proliferation via the canonical transient receptor potential channels 3 and 6.

Since the initial characterization of CaSR expression in the kidney, the majority of studies have supported expression of the CaSR in rat TAL, DT and CD (11, 14, 39, 45). However these studies have failed to agree on the distribution of the CaSR within the CD and also whether expression is present in the PT and glomerulus. RT-PCR on dissected rat nephron segments led to discrepant results with some groups reporting CaSR mRNA expression in the PT (36), and in the glomeruli (11) while others failed to demonstrate CaSR expression in theses nephron segments (11, 45). CaSR protein expression is also controversial, with some authors reporting CaSR expression in the PT (notably

at the apical membrane) using immunofluorescence on sections of frozen rat (34) and mouse kidney (3) while recent studies using human, mouse and rat kidney tissue failed to observe CaSR expression throughout the kidney with the exception of the TAL (22).

The main problems associated with these seemingly contradictory results is that the studies describing the expression of the CaSR have differed in whether they have investigated mRNA or protein expression, used different fixation and/or immunostaining methodologies and have utilized different species. It is plausible that discrepancies between studies have arisen as a consequence of a lack of sensitivity with certain methods or non-specific detection of the CaSR. This study aimed to utilize technical advances in detection methods to gain greater sensitivity and specificity in determining CaSR expression in rat, human and mouse kidney. Using a combination of a branched DNA ISH, immunohistochemistry (using antibodies raised against different epitopes of the CaSR) and a highly sensitive and specific chromogenic *in situ* proximity ligation assay (PLA) method we have demonstrated CaSR expression throughout the kidney. These observations will help to describe the full physiological role of the CaSR in the kidney.

Methods

Tissue Samples

Animal kidney tissue was obtained from adult CD-1 mice or Han Wistar rats, supplied by Harlan (Hillcrest, Leicestershire, UK) or Charles River (Harlow, Essex, UK). Tissue from kidney-specific CaSR-deficient mice was obtained as previously described utilizing transgenic animals expressing Cre recombinase

under the Sine oculis homeobox homolog 2 promoter (Six2-Cre Casr floxed mice) (40). Animals were killed by schedule 1 methods under the UK Animals (Scientific Procedures) Act (1986). Adult normal human kidney cortex tissue used for immunohistochemistry was obtained from the AstraZeneca Global Tissue Bank, compliant with the UK Human Tissue Act (HTA) and AstraZeneca global policies. Adult human kidney tissue used for western blotting was obtained from human kidneys surgically resected at The University Hospital Wales due to renal cell carcinoma (RCC) (Research Ethics Committee approval reference number: 07/WSE04/53) in collaboration with the Wales Cancer Bank. Macroscopically normal kidney cortex tissue was taken from a region separate to the carcinoma.

In situ hybridization

Mouse, rat and human kidneys were fixed in 10% neutral-buffered formalin for 24 to 48h and embedded in paraffin. 5 µm thick sections were cut and ISH was performed using QuantiGene ViewRNA ISH tissue assay (Affymetrix, Santa Clara, CA, USA) according to manufacturer's instructions, with the following modifications: incubation times were 5 min for pretreatment, 20 min for protease digestion, 40 min for PreAmp Hybridization, and 30 min for Amp Hybridization and Label Probe (alkaline phosphatase conjugated probe) incubation. Rat and human specific CaSR probes were obtained from Affymetrix and used at a dilution of 1:40 in the probe diluents provided in the kit. For mouse tissue, a rat probe was used since preliminary experiments showed good species cross-reactivity (rat and mouse CaSR sequences share 94% homology). Sections were mounted using Immu-mount (Thermo Scientific, Waltham, MA, USA).

Negative controls were performed using both a scrambled CaSR probe and an anti-sense probe complementary to the CaSR sense probe.

Immunofluorescence

The antibodies used in this study were screened by immunofluorescence patterns in HEK293 cells stably transfected with the human CaSR (CaSR-HEK), as described previously (24). Cells were fixed in 4% paraformaldehyde in phosphate-buffered saline (PBS), washed and incubated in PBS containing 50 mM NH_4Cl for 10 min. Blocking was performed using 1% bovine serum albumin/0.05% Triton-X 100 in PBS. Primary antibodies (Table 1: Abs 1-8) were incubated overnight at 4ºC at a dilution of 1:100 in blocking buffer. Alexa Fluor 488 or Alexa Fluor 594 fluorescence-dye coupled secondary anti IgG antibodies (Life Technologies, Paisley, UK) were incubated at a dilution of 1:500 in blocking buffer to visualize primary antibody binding. Hoechst 34580 (Life Technologies) was used to stain the nuclei.

Western Blotting

Mouse, rat and human kidney samples and CaSR-HEK or untransfected HEK293 cells were homogenized in modified RIPA buffer (25 mM Tris HCl pH 7.6, 150 mM NaCl, 1% NP40, 0.1% sodium dodecyl sulfate, 1% sodium deoxycholate, 1mM n-ethylmaleimide, 1 mM phenylmethanesulfonylfluoride) containing Halt protease and phosphatase inhibitors (Thermo Scientific). Cell lysis was carried out using a Polytron (Kinematica, Bohemia, NY, USA) homogenizer. Following lysis, homogenates were centrifuged at 10,000 x *g* for 5 min to remove insoluble debris. Protein extracts were quantified using a BCA

protein assay (Thermo Scientific). 20 µg of each extract were subjected to electrophoresis on NuPage® 10% BisTris polyacrylamide gels (Life Technologies). Gels were transferred to nitrocellulose membranes and stained with Ponceau S to confirm even protein loading. Non-specific protein binding was prevented using 5% low-fat dried milk in Tris-buffered saline containing 0.1% Tween (TBST) for 1h at room temperature. Primary antibodies (Table 1: N-term1, N-term2, C-term1 and full length) were added at a dilution of 1:2000 in 5% milk/TBST overnight at 4ºC. A horseradish peroxidase (HRP) conjugated anti-mouse or anti-rabbit secondary antibody (Promega, Madison, WI, USA) was added at a dilution of 1:20,000 or 1:6,000, respectively, in 5% milk/TBST before detection of immunoreactivity with ECL prime using a ChemiDoc MP (Biorad, Hercules, CA, USA).

Immunohistochemistry

Mouse, rat and human kidneys were fixed in 10% neutral-buffered formalin for 24 to 48h and embedded in paraffin. 4 µm thick sections were cut, de-waxed in xylene and rehydrated in ethanol. Antigen retrieval was performed in a Milestone RHS-2 microwave (Milestone, Sorisole, Italy) at 110°C for 2 min in 1 mM ethylenediaminetetraacetic acid (EDTA) buffer, pH 8. Endogenous peroxidase activity was blocked with 3% aqueous hydrogen peroxide for 10min. Immunostaining was carried out using a Labvision autostainer (Labvision, Fremont, CA, USA). Nonspecific binding of the antibody was prevented by incubating slides with background blocker with casein (Menarini, Florence, Italy) for 20 min. Slides were incubated with primary antibodies (Table 1: N-term1, N-term2, full length and C-term1) for 1h at room temperature. Primary antibodies

were detected with X-Cell Plus HRP (Menarini), Envision anti-mouse labeled polymer (DAKO, Glostrup, Denmark) or Ultravision Quanto Mouse on Mouse (Thermo Scientific), and peroxidase was visualized with diamino benzidine (Menarini). Double labeling was performed by incubating tissue sections with antibodies against aquaporin 2 (AQP2, 1:4000, Sigma, St Louis, MO, USA), Tamm Horsfall (1:100, Santa Cruz Biotechnology, Santa Cruz, CA, USA) or the thiazide-sensitive NaCl cotransporter (NCC, 1:500, Millipore, Billerica, MA, USA) as nephron segment markers for 1h at room temperature. AQP2, Tamm Horsfall and NCC were detected by 30 min incubation with goat anti-rabbit antibody conjugated with alkaline phosphatase (Life Technologies), and visualized using Quanto Fast Red Permanent (Thermo Scientific). Sections were counterstained with haematoxylin before dehydration in ethanol, clearing in xylene, and mounting using Hystomount (TAAB Labs, Aldermaston, UK). Negative controls were performed using the appropriate isotype or no primary antibody controls.

Proximity ligation assay

Proximity ligation assays (PLA) were performed using the Duolink® assay with brightfield detection (Sigma) according to the manufacturer's instructions. Briefly, 5 µm thick sections were cut and antigen-retrieval and peroxidase quenching were carried out as described for IHC. Sections were incubated with primary antibody pairs (N-term1/N-term2, N-term1/N-term6, full length/N-term6, C-term1/N-term2, C-term1/N-term6) for 1h at room temperature. Primary antibody pairs were detected by secondary antibodies conjugated with oligonucleotide probes (anti-Rabbit PLA probe Plus and anti-Mouse PLA probe

Minus), incubated for 1h at 37°C. Ligation of the probes was performed by adding oligonucleotides capable of hybridizing to the two probes and ligase enzyme for 30 min at 37°C. Amplification was carried out by adding nucleotides and polymerase enzyme and incubating for 2h at 37°C. Detection was performed by incubation with HRP-conjugated oligonucleotide probes for 1h at room temperature. Peroxidase was then visualized with diamino benzidine (Menarini). Sections were counterstained with haematoxylin before dehydration in ethanol, clearing in xylene, and mounting using Hystomount (TAAB Labs). Negative controls were performed using the appropriate isotype or no primary antibody controls. Additional controls were performed by incubating rat sections with C-term1 and ki67 (1:200, Novus, Littleton, CO, USA) or N-term6 and alpha smooth muscle actin (SMA, 1:3000, Sigma).

Immunoprecipitation

Rat kidney samples were prepared as described for western blotting. Immunoprecipitation was performed using μMACS Protein G MicroBeads and μ Columns (Miltenyi Biotec, Cologne, Germany) according to the manufacturer's instructions. Immunoprecipitation was performed to pull-down CaSR (3 μg, Thermo Scientific), SMA (3 μg, Sigma) and IgG2a (3 μg, Isotype control, Abcam, Cambridge, UK). 20 μl of each immunoprecipitated sample, the lysate pre-clearing flowthrough (negative control) and rat kidney extract (positive control) were subjected to electrophoresis on NuPage® 4-12% BisTris polyacrylamide gels (Life Technologies). Western blotting was performed as described above for SMA (1:2000, Sigma). Controls for western blotting were performed by omission of primary antibody.

259

Results

CaSR mRNA expression

Using ISH, all species showed a high expression of CaSR mRNA in cortical medullary rays (Figure 1A-C) and in the outer medulla (Figure 1D-F), consistent with CaSR expression in the TAL. Lower levels of CaSR mRNA were also detected in the DCT and cortical and medullary CDs, identified by distribution and morphology (Figure 1A-F). There was no signal detected in the papilla of rat and mouse (this region was not present in the human kidney samples). There was also no signal detected in the proximal tubules. Negative controls using either an anti-sense probe or a scrambled probe did not detect any positive signal (Figure 1G-I).

CaSR protein expression

Selection of antibodies

To determine whether the discrepancy in expression patterns obtained in previously published studies could be ascribed to the use of different CaSR antibodies, nine antibodies raised against different regions of the CaSR protein were investigated in this study (Table 1). All antibodies, except N-term6, were initially screened using immunofluorescence on CaSR-HEK cells. For all antibodies, except C-term2, immunofluorescence was detected predominantly at the plasma membrane and in the cytoplasm of the cells (Figure 2). C-term2 showed strong nuclear immunoreactivity, which was considered to be non-specific, particularly as this has not been reported previously, and therefore was excluded from further experiments.

Western Blotting

From the initial immunofluorescence screening process, four antibodies were selected to carry out further studies, based on their recognition of different CaSR epitopes. Antibodies N-term1, N-term3, N-term4, N-term5 all recognize the ADD amino acid sequence within the N-terminal of the CaSR and showed comparable immunofluorescence patterns, therefore only one was selected for further investigation. Out of these, N-term1 was chosen since it has been used most extensively in published studies. N-term2 was selected because it was the only antibody raised against a different epitope within the N-terminal, according to the manufacturer's information; full length and C-term1 antibodies were selected as they were the only available antibodies raised against the full length protein and against the CaSR C-terminal domain, respectively.

In order to further confirm the specificity of these antibodies, western blot profiles were analyzed using mouse, rat and human kidney and CaSR-HEK cell extracts (Figure 3). Immunostaining carried out using N-term1 and N-term2 exhibited CaSR-like immunoreactivity in all 3 species. Conversely, no specific CaSR immunoreactivity was observed in untransfected HEK293 cells immunostained with N-term1 and N-term2. The full length antibody only recognized the CaSR in human tissue and CaSR-HEK cells, consistent with this antibody being raised against a human antigen. C-term1 only cross-reacted with the mouse and rat tissue, consistent with this antibody being raised against a mouse antigen. Unfortunately the antibodies that had been raised against the full-length protein did not cross-react with mouse or rat kidney tissue, while the antibody against the C-terminal region of the CaSR protein did not recognize human kidney tissue. Immunoreactivity of the expected size, that is 140-160

kDa for the glycosylated monomer and/or 260-300 kDa for the mature, fully glycosylated CaSR dimer (43), were observed with all the antibodies. The western blotting profiles revealed some differences between antibodies. Using N-term1, strong immunoreactivity was detected for all the samples; in mouse and rat kidney, immunoreactivity corresponding to the CaSR monomer was detected more strongly than the dimer whereas in human and CaSR-HEK samples the signal distribution was more homogeneous. N-term2 antibody detected preferentially the dimeric form of the CaSR compared to the monomer in all three species. Full length detected very weak CaSR immunoreactivity in human kidney lysate but a stronger signal was obtained in CaSR-HEK lysate. This antibody appeared to detect the monomer and dimer equally well. C-term1 preferentially detected the monomeric form of the CaSR compared with the dimer in both mouse and rat, but it did not cross react with human or CaSR-HEK samples). Thus, further immunohistochemistry studies for each species utilized the following antibodies: N-term1, N-term2 and C-term1 for mouse and rat kidney and N-term1, N-term2 and whole for human kidney.

CaSR protein expression

Having selected suitable antibodies, the CaSR intra-renal distribution was investigated in sections of kidney tissue. Generally, the strongest immunoreactivity was detected in the outer medulla and medullary rays and weak immunoreactivity was detected in the cortex for all the species (Figures 4-6A-F). CaSR immunoreactivity in the different nephron segments was assessed by analysing cellular morphology and co-staining using the CaSR antibodies in combination with established segment-specific markers (Figure 4G-R (mouse),

Figure 5G-R (rat), and Figure 6G-R (human)). In general, CaSR immunoreactivity was found all along the nephron, with a comparable expression pattern across the different species. Specifically, all antibodies detected CaSR immunoreactivity at the basolateral membrane and cytoplasm of the TAL, identified by colocalization with Tamm Horsfall protein (Figures 4-6H,L,P). Consistent with the mRNA distribution by ISH, IHC showed that CaSR immunoreactivity was strongest in the TAL. In addition, CaSR immunoreactivity was consistently detected by all antibodies in the DCT, identified by colocalisation with antibodies directed against NCC (Figures 4-6I,M,Q). In this segment, immunoreactivity was detected apically, basolaterally and within the cytoplasm. CaSR was also present in the connecting tubule (CNT), identified by a combination of morphology and NCC-negative, AQP2-positive cells. In the CDs, identified by a combination of co-localization with AQP2 and morphology (Figures 4-6J,N,R), CaSR expression was heterogeneous. In mouse and rat, CaSR immunoreactivity was found at the basolateral membrane of some cortical CD cells and in the apical membrane and cytoplasm of other cortical CD cells. In CDs in the medulla and papilla, CaSR expression was only observed with N-term2, which showed apical and basolateral immunoreactivity. In human tissue, CaSR immunoreactivity was detected in the cytoplasm and apical and basolateral membranes of most cortical CD cells. Stronger immunoreactivity was detected in a population of CD cells when antibodies N-term1 or N-term2 were used. With N-term2, CaSR immunoreactivity was observed within all cells in the CCDs and therefore all Aqp2 positive cells were also positive for the CaSR. In the inner and outer medullary CDs (MCDs) and also for all the remaining antibodies some cells were CaSR+/Aqp2+, some CaSR+/Aqp2-,

some CaSR-/Aqp2+ and some CaSR-/Aqp2-. CaSR immunoreactivity was very weak in the PT (identified by the presence of brush border) with N-term1, full length and C-term1 (Figures 4-6I,Q). In this segment the intensity of immunostaining signal varied between repeat experiments and in some cases was difficult to distinguish from background levels obtained with isotype controls. However, N-term2 (Figures 4-6M) consistently detected relatively strong immunoreactivity in the cytoplasm and apical membrane of PT cells, which generally increased from the S1 segment down to the S3 segment of the PT. CaSR immunoreactivity was absent or very weak (indistinguishable from background) in the glomeruli and JGA. No specific immunoreactivity was detected in kidney sections from mice deficient in the renal CaSR immunostained with N-term1 or C-term1, or in the corresponding isotype controls (Figure 7). However, N-term2 displayed positive signal throughout the kidney in the KO mice. Some signal was observed in the isotype control for this antibody however the signal with N-term2 appeared to be of greater intensity (data not shown).

Proximity ligation assay

Antibody pairs were initially selected for PLA on their ability to recognise different regions of the CaSR protein, to maximise the chance of signal being observed from the same protein molecule. PLA on mouse and rat kidney using the C-term1/N-term6 antibody pair or in human kidney using the full length/N-term6 antibody pair indicated that, similar to the ISH and IHC results, CaSR expression was greatest in the outer medulla and medullary rays and weaker in the cortex (Figure 8). This distribution clearly demonstrates stronger expression

of the CaSR in the TAL and weaker expression in the DT and CD. Consistent with the ISH and conventional IHC, both positive and negative cells were observed within the CD (Figure 9). Importantly, PLA signal was detected in the PT, with S3 showing higher expression than S1, consistent with conventional IHC using N-term2. In the glomeruli, a positive signal was detected but at a low level, comparable to the proximal tubule expression. The low level of signal combined with the cytoplasmic distribution precluded any determination of positive cell types within the glomerulus. Negative controls showed only the occasional dot of false-positive signal but these were generally associated with areas of the section containing no tissue (*i.e.* lumen of tubules or blood vessels). PLA in rat kidney using other antibody pairs including N-term1/N-term2, N-term1/N-term6, N-term2/C-term1 showed similar results to the C-term1/N-term6 antibody pair (Figure 10). Incubation of rat kidney sections with a C-term1/anti-ki67 antibody pair (used as an antibody to an unrelated protein) also displayed only the occasional dot of positive signal (Figure 11A,B). A further control was conducted using the N-term6 and an anti-SMA antibody pair on rat kidney sections. The CaSR and SMA may interact at a molecular level since both proteins have been demonstrated to interact with filamin (2, 21) and so should result in a positive PLA signal. However, in the kidney, SMA is only expressed in the blood vessels and not in epithelial cells. Accordingly, PLA signal was not observed within cells of the nephron but only in blood vessels (Figure 11C). The specificity of the signal was confirmed by analysing the interaction between the CaSR and SMA with a co-immunoprecipitation assay: SMA expression was observed by western blotting using rat kidney extracts immunoprecipitated with the N-term1 antibody, suggesting that there is an

410 interaction of the CaSR and SMA in vascular smooth muscle cells (Figure 11D).
411 The results from the ISH, IHC and PLA experiments are summarized in Table 2.
412

413 **Discussion**

414 Recent accumulating evidence supports a direct role for the CaSR in the
415 kidney, independent of its indirect, PTH-mediated actions. Yet, its intrarenal
416 distribution is still controversial. Pharmacological CaSR modulators are either in
417 use in the clinic (calcimimetics) (6) or are currently being developed for the
418 treatment of genetic hypocalcemia with hypercalciuria (autosomal dominant
419 hypocalcemia, calcilytics) (27). Therefore, the aim of the current study was to
420 determine, conclusively and unequivocally, the intra-renal distribution of the
421 CaSR using the most sensitive and specific detection methods available for
422 examining large numbers of each renal cell type across different species. This
423 knowledge is essential to fully elucidate the role of the CaSR in the kidney and
424 key to discriminating between CaSR-dependent and CaSR-independent roles of
425 physiological and pharmacological CaSR modulators in the kidney. Because
426 some of the discrepancies were previously ascribed to species differences, we
427 assessed both CaSR mRNA and protein localisation in mouse, rat and human
428 kidneys. For protein localisation, we tested a wide variety of commercially and
429 non-commercially available antibodies, raised against different regions of the
430 CaSR protein. The initial screening of antibodies using immunofluorescence
431 indicated that seven out of the eight investigated antibodies specifically
432 detected the CaSR in positively transfected cells, but not in sham-transfected
433 cells. This result suggests that false positive protein detection is unlikely to be a
434 major cause of discrepancies between studies. One antibody, C-term2, did fail

this initial screen although this could be due to an inability of this antibody to detect the correct antigen following paraformaldehyde fixation.

Consistent with previous reports, western blotting showed the expected heterogeneity of CaSR species present in the kidney given by the combination of the nude protein, the high mannose and fully mature monomeric and dimeric CaSR (4, 5, 43). Interestingly, the battery of antibodies tested showed different profiles for the detection of the different molecular species. Despite the different western blotting profiles, there was generally a consistent pattern of protein expression by immunohistochemistry, regardless of the antibody used. N-term2 displayed a slightly different profile by immunohistochemistry compared to N-term1 and C-term1, notably a more intense expression of the CaSR in proximal tubules. By western blotting this antibody was the only antibody to predominantly detect dimeric forms of the CaSR. Since the dimerization is an essential step in the maturation of the CaSR(31), it is possible that N-term2 has a greater sensitivity to detect more mature forms of this receptor than the remaining antibodies. Alternatively, this antibody may display some non-specific binding in FFPE tissue in addition to CaSR binding. The lack of specificity of this antibody in FFPE tissue is supported by the positive signal obtained in the CaSR deficient kidney tissue. In contrast, the specificity of the signal detected by the N-term1 and N-term 2 antibodies was confirmed in mice with selective CaSR ablation from the kidney.

Loop of Henle and distal tubule

The highest CaSR mRNA and protein expression were observed basolaterally in the TAL, the only segment unanimously recognized to express the CaSR (3,

10, 22, 34, 40, 45). Functional studies have shown that the CaSR inhibits PTH-induced transcellular divalent cation reabsorption in this nephron segment (26). Also, in this nephron segment CaSR activation directly inhibits paracellular divalent cation reabsorption through PTH-independent processes (22, 40). These processes are associated with the modulation of transepithelial potential difference through the inhibition of Na-K-Cl cotransporter 2 (NKCC2) activity (40) and with the epigenetic regulation of micro RNA controlling claudin 14 expression (17, 40). Expression of both CaSR mRNA and protein was also observed in the DCT, and functional expression of CaSR in DCT has been previously linked to regulation of Ca reabsorption from the pro-urine via TRPV5 (41) and to regulation of Kir4.1 (19).

Collecting ducts

Within the collecting ducts, all techniques demonstrated greatest CaSR expression in CCD compared with outer and inner MCDs. IHC with N-term2 and PLA demonstrated a lower expression of CaSR in MCDs that was not observed with other techniques. With the exception of IHC with N-term2, all methods (including PLA) revealed that only a proportion of CCDs were positive for CaSR expression (approximately 30%). Whilst it cannot be ruled out that N-term2 shows greater sensitivity than all the other techniques, it is more likely that this antibody is either recognising non-specific signal in addition to the CaSR in FFPE tissue, or it is the only method to detect a specific form of the receptor. Given the significantly greater signal for the dimer observed by western blotting with this antibody (compared to the others), the latter explanation is a possibility. CaSR positive CD cells could not be attributed to being either principal or intercalated cells since populations of CaSR+/AQP2+,

CaSR+/Aqp2-, CaSR-/Aqp2+ and CaSR-/Aqp2- were clearly observed. In agreement with the original description of CaSR localisation in CCDs (34), heterogeneous expression within the cytoplasm, apical and/or basolateral membranes was observed in the current study. Characterisation of the cell types in the study by Riccardi et al demonstrated CaSR expression in some, but not all, type A intercalated cells (34). Functionally this is supported by studies in TRPV5$^{-/-}$ mice, where the CaSR is activated by increased urinary Ca^{2+} levels, which triggers urinary acidification by increasing the H^{+}-ATPase activity (33). Principal cell expression is also suggested by studies demonstrating that activation of an apical CaSR expression in CDs is specifically involved in reduction of AVP-elicited osmotic water permeability via reduction of Aqp2 (9, 32, 39). Recently, pH-sensitive CaSR expression was described as being restricted to the basolateral membrane of type B intercalated cells (46), although the images presented appeared to show weaker staining in N-term2 and anion exchanger 1 positive cells. Our data support the presence of the CaSR in both principal and intercalated cells, with significant heterogeneity in expression levels and also polarity. Further work is needed to elucidate the reasons behind the restricted expression of the CaSR to subpopulations of these different cell types.

Proximal tubule

The proximal tubule is the nephron segment where greatest discrepancies in CaSR expression have been reported between studies. Our data with IHC and ISH was inconclusive since only one antibody, N-term2, convincingly showed proximal tubule expression. Since this antibody also showed signal in the CaSR deficient mice, this staining was likely to be non-specific. The level of staining

with the other antibodies and also with ISH varied slightly between repeat experiments and was difficult to distinguish above possible background staining. However, using PLA we were specifically able to detect a low level of CaSR expression in the proximal tubule. This method confers greater specificity than conventional IHC since specific detection of the same molecule by a pair of antibodies is necessary to produce a positive signal. In addition the method includes an amplification step, further increasing the sensitivity over conventional methods. This finding supports functional studies demonstrating that, in mice, activation of the CaSR by increased luminal gadolinium blocks the inhibitory effect of PTH in phosphate absorption in the proximal tubule (3) and also that in both rats and mice, activation of the CaSR by increased luminal calcium concentration enhances fluid reabsorption in the proximal tubule (10). Finally, a recent study has demonstrated expression of a functional CaSR at the apical membrane of conditionally immortalized proximal tubular epithelial cells obtained from healthy urine (12).

Glomerulus

The majority of studies addressing CaSR expression in the kidney have failed to observe localisation within the glomerulus. In the current study, PLA was also the only technique to convincingly demonstrate CaSR expression within glomeruli. Functional effects of the CaSR have been described in both podocytes (28) and in cultured mesangial cells (20, 25). Interestingly our results showed considerable variation in CaSR expression within glomeruli from the same animal, even between adjacent glomeruli. The reason for this is not currently understood but could reflect differences in functional activity of individual glomeruli at a given time.

In conclusion, this study has demonstrated CaSR expression throughout the nephron and in glomeruli, although the level of expression varied considerably between different cell types. A summary of the distribution and roles of the CaSR in the kidney is shown in Figure 12. In contrast, there was little variation in the expression pattern between mouse, rat and human, suggesting conserved functions of the receptor between these species. The highest CaSR expression was detected in the TAL, where this receptor regulates Ca^{2+} reabsorption. Besides, the CaSR was detected in different cell types from other nephron segments with significantly lower expression compared with the abundantly expressing cells of the TAL. These data corroborate previous functional studies showing CaSR expression in cell types where functional effects have been demonstrated specifically in the PT, DCT and CD. Furthermore, this information will prove valuable for studies aimed at testing the ability of calcimimetics in transplant patients (44) and of calcilytics for the treatment of hypercalciuria and nephrocalcinosis (27).

Acknowledgements

This work was supported by a Marie Curie Initial Training Network ("Multifaceted CaSR", to SAP and DR). The authors would like to thank Sonia Eckersley for technical assistance with proximity ligation assays.

Figure Legends

Table 1. Details of antibodies used in the study.

*N-term1 is a monoclonal antibody produced using the 5C10, ADD clone and commercialized by different companies including Abcam, Thermo-Scientific, Novus Bio, Genetex (Irvine, CA, USA) and Acris (Herford, Germany). † Anaspec, Fremont, USA. ‡ LS Bio, Seattle, USA.

Table 2. Summary of the localization of the CaSR observed by ISH, IHC and PLA.

Figure 1. Localization of CaSR mRNA in mouse, rat and human kidney. Photomicrographs of *in situ* hybridization using probes directed against CaSR in cortical sections of mouse (A), rat (B) and human (C) kidney and in medullary sections of mouse (D) and rat (E) and human (E) kidney. CaSR signal (in red) corresponds to fast red staining and nuclei are counterstained with haematoxylin (blue). Photomicrographs of negative controls for the *in situ* hybridization in mouse (G), rat (H) and human (I) cortical sections. Negative controls were performed by incubation with anti-sense probes (rat) or omission of CaSR probe (mouse and human). Scale bar = 50 µm. Arrows indicate stronger staining, consistent with TAL expression; arrowheads indicate weaker expression, consistent with DT and CD. Pictures are representative of three (mouse and rat) or two (human) independent experiments.

Figure 2. CaSR immunolocalization in HEK293 cells stably expressing the human CaSR. Immunofluorescence using eight different anti-CaSR antibodies, N-term1 (Abcam), N-term2 (Anaspec), N-term3 (W. Chang), N-term4 (W.

Chang), N-term5 (W. Chang), C-term1 (W. Chang), C-term2 (Lifespan), full length (Novus). Scale bar = 30 μm.

Figure 3. Western blotting profile for the different CaSR antibodies used in this study. Western blotting using N-term1 (Thermo), N-term2 (Anaspec), full length (Novus) and C-term1 (W. Chang) antibodies in mouse (Ms), rat (Rt) and human (Hu) kidney and CaSR-HEK (Hk) extracts (A). CaSR monomers and dimers are detected at 140-160 kDa and 260-300 kDa, respectively. Western blotting negative controls performed by omitting the primary antibodies (B). Western blotting using N-term1 and N-term2 antibodies in CaSR-HEK (Hk) and in untransfected HEK (Hk-Ø) cell extracts (C).

Figure 4. CaSR immunolocalization in mouse kidney sections. Photomicrographs of mouse cortical kidney sections immunostained with the CaSR antibodies N-term1 (Thermo; A), N-term2 (Anaspec, B) and C-term1 (W. Chang, C). Photomicrographs of mouse medullary kidney sections immunostained with the CaSR antibodies N-term1 (D), N-term2 (E) and C-term1 (F). Positive CaSR signal corresponds to immunoperoxidase staining (brown) and nuclei are counterstained with haematoxylin (blue). Arrows indicate stronger signal consistent with TAL and arrowheads indicate weaker signal consistent with DCT and CD. Photomicrographs showing CaSR immunoreactivity in the PT, identified by the presence of brush border in kidney sections immunostained with N-term1 (G), N-term2 (K) and C-term1 (O). Asterisk indicates the PT. Photomicrographs showing CaSR immunoreactivity in the TAL, identified by dual staining with Tamm Horsfall protein in kidney

606 sections immunostained with N-term1 (H), N-term2 (L) and C-term1 (P).
607 Photomicrographs showing CaSR immunoreactivity in the DCT, identified by
608 dual staining with the thiazide-sensitive Na-Cl cotransporter (NCC) in kidney
609 sections immunostained with N-term1 (I), N-term2 (M) and C-term1 (Q).
610 Photomicrographs showing CaSR immunoreactivity in the CD, identified by dual
611 staining with Aquaporin-2 (AQP2) in kidney sections immunostained with N-
612 term1 (J), N-term2 (N) and C-term1 (R). Nephron segment marker signal
613 corresponds to (red) fast red staining. Photomicrographs for the negative
614 controls for N-term1 (S), N-term2 (T) and C-term1 (U), performed by omitting
615 the primary antibody. Scale bar = 100 μm for pictures A-F and S-U and 50 μm
616 for pictures G-R.
617

618 **Figure 5. CaSR immunolocalization in rat kidney sections.**
619 Photomicrographs of rat cortical kidney sections immunostained with the CaSR
620 antibodies N-term1 (Thermo; A), N-term2 (Anaspec, B) and C-term1 (W.
621 Chang, C). Photomicrographs of rat medullary kidney sections immunostained
622 with the CaSR antibodies N-term1 (D), N-term2 (E) and C-term1 (F). Positive
623 CaSR signal corresponds to immunoperoxidase staining (brown) and nuclei are
624 counterstained with haematoxylin (blue). Arrows indicate stronger signal
625 consistent with TAL and arrowheads indicate weaker signal consistent with DCT
626 and CD. Photomicrographs showing CaSR immunoreactivity in the PT,
627 identified by the presence of brush border in kidney sections immunostained
628 with N-term1 (G), N-term2 (K) and C-term1 (O). Asterisk indicates the PT.
629 Photomicrographs showing CaSR immunoreactivity in the TAL, identified by
630 dual staining with Tamm Horsfall protein in kidney sections immunostained with

N-term1 (H), N-term2 (L) and C-term1 (P). Photomicrographs showing CaSR immunoreactivity in the DCT, identified by dual staining with the thiazide-sensitive Na-Cl cotransporter (NCC) in kidney sections immunostained with N-term1 (I), N-term2 (M) and C-term1 (Q). Photomicrographs showing CaSR immunoreactivity in the CD, identified by dual staining with Aquaporin-2 (AQP2) in kidney sections immunostained with N-term1 (J), N-term2 (N) and C-term1 (R). Nephron segment marker signal corresponds to (red) fast red staining. Photomicrographs for the negative controls for N-term1 (S), N-term2 (T) and C-term1 (U), performed by incubation with the corresponding isotype controls. Scale bar = 100 μm for pictures A-F and S-U and 50 μm for pictures G-R.

Figure 6. CaSR immunolocalization in human kidney sections.

Photomicrographs of human cortical kidney sections immunostained with the CaSR antibodies N-term1 (Thermo; A), N-term2 (Anaspec, B) and Full length (Novus, C). Photomicrographs of human medullary kidney sections immunostained with the CaSR antibodies N-term1 (D), N-term2 (E) and Full length (F). Positive CaSR signal corresponds to immunoperoxidase staining (brown) and nuclei are counterstained with haematoxylin (blue). Arrows indicate stronger signal consistent with TAL and arrowheads indicate weaker signal consistent with DCT and CD. Photomicrographs showing CaSR immunoreactivity in the PT, identified by the presence of brush border in kidney sections immunostained with N-term1 (G), N-term2 (K) and Full length (O). Asterisk indicates the PT. Photomicrographs showing CaSR immunoreactivity in the TAL, identified by dual staining with Tamm Horsfall protein in kidney sections immunostained with N-term1 (H), N-term2 (L) and Full length (P).

Photomicrographs showing CaSR immunoreactivity in the DCT, identified by dual staining with the thiazide-sensitive Na-Cl cotransporter (NCC) in kidney sections immunostained with N-term1 (I), N-term2 (M) and Full length (Q). Photomicrographs showing CaSR immunoreactivity in the CD, identified by dual staining with Aquaporin-2 (AQP2) in kidney sections immunostained with N-term1 (J), N-term2 (N) and Full length (R). Nephron segment marker signal corresponds to (red) fast red staining. Photomicrographs for the negative controls for N-term1 (S), N-term2 (T) and Full length (U), performed by omitting the primary antibody. Scale bar = 100 μm for pictures A-F and S-U and 50 μm for pictures G-R.

Figure 7. CaSR immunostaining in mice lacking the renal CaSR. Photomicrographs of cortical kidney sections from WT mice immunostained with the CaSR antibodies N-term1 (A) and C-term1 (B) or with the corresponding isotype control (C). Photomicrographs of cortical kidney sections from mice lacking the renal CaSR (D-F) immunostained with the CaSR antibodies N-term1 (D) and C-term1 (E) or with the corresponding isotype control (F). Positive signal corresponds to immunoperoxidase staining (brown) and nuclei are counterstained with haematoxylin (blue). Scale bar = 100μm.

Figure 8. CaSR detection by proximity ligation assay in mouse, rat and human kidney. Photomicrographs of CaSR immunolocalization by proximity ligation assay in mouse (A), rat (C) and human (E) cortical kidney sections. Immunoperoxidase staining (brown dots) indicates the proximity between the epitopes detected by the C-term1/N-term6 antibody pair in mouse and rat

sections and by the full length/N-term6 antibody pair in human sections. Photomicrographs of the negative controls performed by incubation with isotype control or omission of primary antibody (mouse, B; rat, D; human, F). Arrow indicates TAL and asterisk indicates PT. Scale bar = 50μm.

Figure 9. CaSR expression in rat kidney CD. Photomicrographs of CaSR mRNA expression in CCD detected by ISH (A). Positive signal (as detected by ISH) corresponds to fast red staining. Photomicrographs of CaSR protein expression in CCD detected by IHC with N-term1 (Thermo, B), N-term2 (Anaspec, C), C-term1 (W. Chang, D) or PLA with C-term1/N-term6 (Alomone, E). Photomicrographs of CaSR protein expression in outer MCD, detected by PLA with C-term1/N-term6 (F). Positive signal corresponds to immunoperoxidase staining (brown) and nuclei are counterstained with haematoxylin (blue) in IHC and PLA images. Scale bar = 50 μm.

Figure 10. CaSR detection by proximity ligation assay in rat kidney. Photomicrographs of proximity ligation assay using the CaSR antibody pair N-term1/N-term6 in outer (A) and inner (B) cortical kidney sections. Photomicrographs of proximity ligation assay using the CaSR antibody pair N-term1/N-term2 in outer (C) and inner (D) cortical kidney sections. Photomicrographs of proximity ligation assay using the CaSR antibody pair N-term2/C-term1 in outer (E) and inner (F) cortical kidney sections, (E). Positive staining corresponds to immunoperoxidase staining (brown dots). Asterisks indicate proximal tubules. Scale bar = 50 μm.

Figure 11. Controls for CaSR detection by proximity ligation assay in rat kidney. Photomicrograph of the negative control for the proximity ligation assay using the C-term1/anti-ki67 antibody pair in an outer cortical kidney section (A). Photomicrograph of the negative control for the proximity ligation assay using the N-term6/anti-SMA antibody pair in an outer cortical kidney section (B). Photomicrograph of the proximity ligation assay signal observed using the N-term6/anti-SMA antibody pair in a renal blood vessel (C). Positive staining corresponds to immunoperoxidase staining (brown dots). Scale bar = 50 μm for the outer cortex pictures and 100 μm for the magnified blood vessel. The interaction between SMA and CaSR in blood vessels was confirmed by co-immunoprecipitation: proteins from rat kidney extracts were immunoprecipitated with N-term1, anti-SMA or an IgG control. The immunoprecipitated proteins, together with the buffer used to pre-clear the assay columns (pc) and total protein extracts (Rt) were analysed by western blotting with an anti-SMA antibody (D). Control for the western blotting was performed by omitting the primary antibody (E). SMA MW = 42 kDa.

Figure 12. Distribution and roles of the CaSR in the kidney. Diagrams representing the intra-renal distribution (left) and polarity (right) of the CaSR observed in this study, which is comparable in mouse, rat and human kidney. The strongest CaSR expression was observed in the TAL (dark grey) using in situ hybridization, immunohistochemistry and proximity ligation assay, however the CaSR was also consistently detected in the DCT/CNT and CD by these three techniques (medium grey). Additionally, weak CaSR expression was detected in the glomerulus and PT using a proximity ligation assay (light gray). The diagrams also summarize functional roles previously reported for the CaSR

in the different nephron segments. PT, proximal tubule; tDL, thin descending limb; tAL, thin ascending limb; TAL, thick ascending limb; DCT, distal convoluted tubule; CNT connecting tubule; CD, collecting duct; TRPC 3/6, transient receptor potential cation channel 3/6; PTH1R, parathyroid hormone 1 receptor; NHE3, sodium–hydrogen exchanger 3; NKCC2, Na-K-Cl cotransporter 2; ROMK, renal outer medullary K+ channel; TRPV5, transient receptor potential vanilloid 5; PMCA, plasma membrane Ca2+-ATPase; Kir 4.1, inward rectifying potassium channel 4.1; AQP2, aquaporin 2.

References

1. **Atchison DK, Ortiz-Capisano MC, and Beierwaltes WH**. Acute activation of the calcium-sensing receptor inhibits plasma renin activity in vivo. *American Journal of Physiology - Regulatory, Integrative and Comparative Physiology* 299: R1020-R1026, 2010.
2. **Awata H, Huang C, Handlogten ME, and Miller RT**. Interaction of the calcium-sensing receptor and filamin, a potential scaffolding protein. *J Biol Chem* 276: 34871-34879, 2001.
3. **Ba J, Brown D, and Friedman PA**. Calcium-sensing receptor regulation of PTH-inhibitable proximal tubule phosphate transport. *Am J Physiol Renal Physiol* 285: F1233-1243, 2003.
4. **Bai M, Quinn S, Trivedi S, Kifor O, Pearce SH, Pollak MR, Krapcho K, Hebert SC, and Brown EM**. Expression and characterization of inactivating and activating mutations in the human Ca2+o-sensing receptor. *J Biol Chem* 271: 19537-19545, 1996.
5. **Bai M, Trivedi S, and Brown EM**. Dimerization of the extracellular calcium-sensing receptor (CaR) on the cell surface of CaR-transfected HEK293 cells. *J Biol Chem* 273: 23605-23610, 1998.
6. **Block GA, Martin KJ, de Francisco AL, Turner SA, Avram MM, Suranyi MG, Hercz G, Cunningham J, Abu-Alfa AK, Messa P, Coyne DW, Locatelli F, Cohen RM, Evenepoel P, Moe SM, Fournier A, Braun J, McCary LC, Zani VJ, Olson KA, Drueke TB, and Goodman WG**. Cinacalcet for secondary hyperparathyroidism in patients receiving hemodialysis. *N Engl J Med* 350: 1516-1525, 2004.
7. **Brown EM, Gamba G, Riccardi D, Lombardi M, Butters R, Kifor O, Sun A, Hediger MA, Lytton J, and Hebert SC**. Cloning and characterization of an extracellular Ca(2+)-sensing receptor from bovine parathyroid. *Nature* 366: 575-580, 1993.
8. **Bukoski RD, Bian K, Wang Y, and Mupanomunda M**. Perivascular sensory nerve Ca2+ receptor and Ca2+-induced relaxation of isolated arteries. *Hypertension* 30: 1431-1439, 1997.

9. **Bustamante M, Hasler U, Leroy V, de Seigneux S, Dimitrov M, Mordasini D, Rousselot M, Martin P-Y, and Féraille E**. Calcium-sensing Receptor Attenuates AVP-induced Aquaporin-2 Expression via a Calmodulin-dependent Mechanism. *J Am Soc Nephrol* 19: 109-116, 2008.
10. **Capasso G, Geibel PJ, Damiano S, Jaeger P, Richards WG, and Geibel JP**. The calcium sensing receptor modulates fluid reabsorption and acid secretion in the proximal tubule. *Kidney Int* 84: 277-284, 2013.
11. **Caride AJ, Chini EN, Homma S, Dousa TP, and Penniston JT**. mRNAs coding for the calcium-sensing receptor along the rat nephron: effect of a low-phosphate diet. *Kidney Blood Press Res* 21: 305-309, 1998.
12. **Di Mise A, Tamma G, Ranieri M, Svelto M, van den Heuvel B, Levtchenko EN, and Valenti G**. Conditionally Immortalized Human Proximal-Tubular Epithelial Cells isolated from the urine of a healthy subject express functional Calcium Sensing Receptor. *Am J Physiol Renal Physiol* ajprenal.00352.02014, 2015.
13. **Farajov EI, Morimoto T, Aslanova UF, Kumagai N, Sugawara N, and Kondo Y**. Calcium-sensing receptor stimulates luminal K+-dependent H+ excretion in medullary thick ascending limbs of Henle's loop of mouse kidney. *Tohoku J Exp Med* 216: 7-15, 2008.
14. **Ferreira MCdJ, Héliès-Toussaint C, Imbert-Teboul M, Bailly C, Verbavatz J-M, Bellanger A-C, and Chabardès D**. Co-expression of a Ca2+-inhibitable Adenylyl Cyclase and of a Ca2+-sensing Receptor in the Cortical Thick Ascending Limb Cell of the Rat Kidney: INHIBITION OF HORMONE-DEPENDENT cAMP ACCUMULATION BY EXTRACELLULAR Ca2+. *J Biol Chem* 273: 15192-15202, 1998.
15. **Gama L, Baxendale-Cox LM, and Breitwieser GE**. Ca2+-sensing receptors in intestinal epithelium. *Am J Physiol* 273: C1168-1175, 1997.
16. **Garrett JE, Tamir H, Kifor O, Simin RT, Rogers KV, Mithal A, Gagel RF, and Brown EM**. Calcitonin-secreting cells of the thyroid express an extracellular calcium receptor gene. *Endocrinology* 136: 5202-5211, 1995.
17. **Gong Y, Renigunta V, Himmerkus N, Zhang J, Renigunta A, Bleich M, and Hou J**. Claudin-14 regulates renal Ca(+)(+) transport in response to CaSR signalling via a novel microRNA pathway. *EMBO J* 31: 1999-2012, 2012.
18. **House MG, Kohlmeier L, Chattopadhyay N, Kifor O, Yamaguchi T, Leboff MS, Glowacki J, and Brown EM**. Expression of an extracellular calcium-sensing receptor in human and mouse bone marrow cells. *J Bone Miner Res* 12: 1959-1970, 1997.
19. **Huang C, Sindic A, Hill CE, Hujer KM, Chan KW, Sassen M, Wu Z, Kurachi Y, Nielsen S, Romero MF, and Miller RT**. Interaction of the Ca2+-sensing receptor with the inwardly rectifying potassium channels Kir4.1 and Kir4.2 results in inhibition of channel function. *Am J Physiol Renal Physiol* 292: F1073-1081, 2007.
20. **Kwak JO, Kwak J, Kim HW, Oh KJ, Kim YT, Jung SM, and Cha SH**. The extracellular calcium sensing receptor is expressed in mouse mesangial cells and modulates cell proliferation. *Exp Mol Med* 37: 457-465, 2005.
21. **Lebart MC, Mejean C, Casanova D, Audemard E, Derancourt J, Roustan C, and Benyamin Y**. Characterization of the actin binding site on smooth muscle filamin. *J Biol Chem* 269: 4279-4284, 1994.
22. **Loupy A, Ramakrishnan SK, Wootla B, Chambrey R, de la Faille R, Bourgeois S, Bruneval P, Mandet C, Christensen EI, Faure H, Cheval L, Laghmani K, Collet C, Eladari D, Dodd RH, Ruat M, and Houillier P**. PTH-independent regulation of blood calcium concentration by the calcium-sensing receptor. *J Clin Invest* 122: 3355-3367, 2012.
23. **Maillard MP, Tedjani A, Perregaux C, and Burnier M**. Calcium-sensing receptors modulate renin release in vivo and in vitro in the rat. *J Hypertens* 27: 1980-1987, 2009.
24. **Maldonado-Perez D, Breitwieser GE, Gama L, Elliott AC, Ward DT, and Riccardi D**. Human calcium-sensing receptor can be suppressed by antisense sequences. *Biochem Biophys Res Commun* 311: 610-617, 2003.

25. **Meng K, Xu J, Zhang C, Zhang R, Yang H, Liao C, and Jiao J**. Calcium sensing receptor modulates extracellular calcium entry and proliferation via TRPC3/6 channels in cultured human mesangial cells. *PLoS One* 9: e98777, 2014.
26. **Motoyama HI, and Friedman PA**. Calcium-sensing receptor regulation of PTH-dependent calcium absorption by mouse cortical ascending limbs. *Am J Physiol Renal Physiol* 283: F399-F406, 2002.
27. **Nemeth EF, and Shoback D**. Calcimimetic and calcilytic drugs for treating bone and mineral-related disorders. *Best Pract Res Clin Endocrinol Metab* 27: 373-384, 2013.
28. **Oh J, Beckmann J, Bloch J, Hettgen V, Mueller J, Li L, Hoemme M, Gross ML, Penzel R, Mundel P, Schaefer F, and Schmitt CP**. Stimulation of the calcium-sensing receptor stabilizes the podocyte cytoskeleton, improves cell survival, and reduces toxin-induced glomerulosclerosis. *Kidney Int* 80: 483-492, 2011.
29. **Ortiz-Capisano MC, Ortiz PA, Garvin JL, Harding P, and Beierwaltes WH**. Expression and function of the calcium-sensing receptor in juxtaglomerular cells. *Hypertension* 50: 737-743, 2007.
30. **Ortiz-Capisano MC, Reddy M, Mendez M, Garvin JL, and Beierwaltes WH**. Juxtaglomerular cell CaSR stimulation decreases renin release via activation of the PLC/IP(3) pathway and the ryanodine receptor. *Am J Physiol Renal Physiol* 304: F248-256, 2013.
31. **Pidasheva S, Grant M, Canaff L, Ercan O, Kumar U, and Hendy GN**. Calcium-sensing receptor dimerizes in the endoplasmic reticulum: biochemical and biophysical characterization of CASR mutants retained intracellularly. *Hum Mol Genet* 15: 2200-2209, 2006.
32. **Procino G, Mastrofrancesco L, Tamma G, Lasorsa DR, Ranieri M, Stringini G, Emma F, Svelto M, and Valenti G**. Calcium-sensing receptor and aquaporin 2 interplay in hypercalciuria-associated renal concentrating defect in humans. An in vivo and in vitro study. *PLoS One* 7: e33145, 2012.
33. **Renkema KY, Velic A, Dijkman HB, Verkaart S, van der Kemp AW, Nowik M, Timmermans K, Doucet A, Wagner CA, Bindels RJ, and Hoenderop JG**. The calcium-sensing receptor promotes urinary acidification to prevent nephrolithiasis. *J Am Soc Nephrol* 20: 1705-1713, 2009.
34. **Riccardi D, Hall AE, Chattopadhyay N, Xu JZ, Brown EM, and Hebert SC**. Localization of the extracellular Ca2+/polyvalent cation-sensing protein in rat kidney. *American Journal of Physiology - Renal Physiology* 274: F611-F622, 1998.
35. **Riccardi D, Hall AE, Chattopadhyay N, Xu JZ, Brown EM, and Hebert SC**. Localization of the extracellular Ca2+/polyvalent cation-sensing protein in rat kidney. *Am J Physiol* 274: F611-622, 1998.
36. **Riccardi D, Lee WS, Lee K, Segre GV, Brown EM, and Hebert SC**. Localization of the extracellular Ca(2+)-sensing receptor and PTH/PTHrP receptor in rat kidney. *Am J Physiol* 271: F951-956, 1996.
37. **Riccardi D, Park J, Lee WS, Gamba G, Brown EM, and Hebert SC**. Cloning and functional expression of a rat kidney extracellular calcium/polyvalent cation-sensing receptor. *Proc Natl Acad Sci U S A* 92: 131-135, 1995.
38. **Ruat M, Molliver ME, Snowman AM, and Snyder SH**. Calcium sensing receptor: molecular cloning in rat and localization to nerve terminals. *Proc Natl Acad Sci U S A* 92: 3161-3165, 1995.
39. **Sands JM, Naruse M, Baum M, Jo I, Hebert SC, Brown EM, and Harris HW**. Apical extracellular calcium/polyvalent cation-sensing receptor regulates vasopressin-elicited water permeability in rat kidney inner medullary collecting duct. *J Clin Invest* 99: 1399-1405, 1997.
40. **Toka HR, Al-Romaih K, Koshy JM, DiBartolo S, Kos CH, Quinn SJ, Curhan GC, Mount DB, Brown EM, and Pollak MR**. Deficiency of the Calcium-Sensing Receptor in the Kidney Causes Parathyroid Hormone–Independent Hypocalciuria. *J Am Soc Nephrol* 23: 1879-1890, 2012.

41. **Topala CN, Schoeber JPH, Searchfield LE, Riccardi D, Hoenderop JGJ, and Bindels RJM**. Activation of the Ca2+-sensing receptor stimulates the activity of the epithelial Ca2+ channel TRPV5. *Cell Calcium* 45: 331-339, 2009.

42. **Wang R, Xu C, Zhao W, Zhang J, Cao K, Yang B, and Wu L**. Calcium and polyamine regulated calcium-sensing receptors in cardiac tissues. *Eur J Biochem* 270: 2680-2688, 2003.

43. **Ward DT, Brown EM, and Harris HW**. Disulfide Bonds in the Extracellular Calcium-Polyvalent Cation-sensing Receptor Correlate with Dimer Formation and Its Response to Divalent Cations in Vitro. *J Biol Chem* 273: 14476-14483, 1998.

44. **Weekers L, de Tullio P, Bovy C, Poma L, Maree R, Bonvoisin C, Defraigne JO, Krzesinski JM, and Jouret F**. Activation of the calcium-sensing receptor before renal ischemia/reperfusion exacerbates kidney injury. *Am J Transl Res* 7: 128-138, 2015.

45. **Yang T, Hassan S, Huang YG, Smart AM, Briggs JP, and Schnermann JB**. Expression of PTHrP, PTH/PTHrP receptor, and Ca(2+)-sensing receptor mRNAs along the rat nephron. *Am J Physiol* 272: F751-758, 1997.

46. **Yasuoka Y, Sato Y, Healy J, Nonoguchi H, and Kawahara K**. pH-sensitive expression of calcium-sensing receptor (CaSR) in type-B intercalated cells of the cortical collecting ducts (CCD) in mouse kidney. *Clin Exp Nephrol* 1-12, 2014.

Antibody	Manufacturer	Reactivity	Epitope		Host	Clone	IHC Dilution
			Species	Region			
N-term1	**Abcam (ab19347) / Thermo (MA1-934) ***	**Mouse, Rat, Human**	**Human**	**N-term (ADD)** **N'-ADDDYGRPGIEKFREEAEERDI-C'**	**Mouse**	**Mono**	**1:500**
N-term2	**Anaspec † (53286)**	**Mouse, Rat, Human**	**Rat**	**N-term**	**Rabbit**	**Poly**	**1:500**
N-term3	W. Chang (custom made)	Mouse, Rat, Human	Human	N-term (ADD) N'-DYGRPGIEKFREEAEE-C'	Mouse	Mono	Not tested
N-term4	W. Chang (custom made)	Mouse, Rat, Human	Human	N-term (ADD) N'-DYGRPGIEKFREEAEE-C'	Mouse	Mono	Not tested
N-term5	W. Chang (custom made)	Mouse, Rat, Human	Human	N-term (ADD) N'-ADDDYGRPGIEKFREEAEERDI-C'	Rabbit	Poly	Not tested
N-term-6	Alomone (ACR-004)	Mouse, Rat, Human	Human	N-term (ADD)	Rabbit	Poly	1:500
C-term1	**W. Chang (custom made)**	**Mouse, Rat**	**Mouse**	**C-term** **N'-NSEDRFPQPERQKQ-C'**	**Mouse**	**Mono**	**1:150**
C-term2	LS Bio‡ (LS-C117834)	Mouse, Rat, Human	Human	C-term aa854-903	Rabbit	Poly	Not tested
Full length	**Novus Bio (H00000846-B01P)**	**Human**	**Human**	**Full length**	**Mouse**	**Poly**	**1:75**

		Glomerulus	PT	TAL	DCT	CNT	CCD	MCD
ISH		-	-	++++	++	+	++	+
IHC	N-term1	-	+/-	++++	++	+	++	-
	N-term2	-	++	++++	++	++	++	++
	Full length	-	+/-	++++	++	+	++	-
	C-term1	-	+/-	++++	++	+	++	-
PLA	C-term1/N-term6	+	+	++++	++	+	++	+
	Full length/N-term6	+	+	++++	++	+	++	+

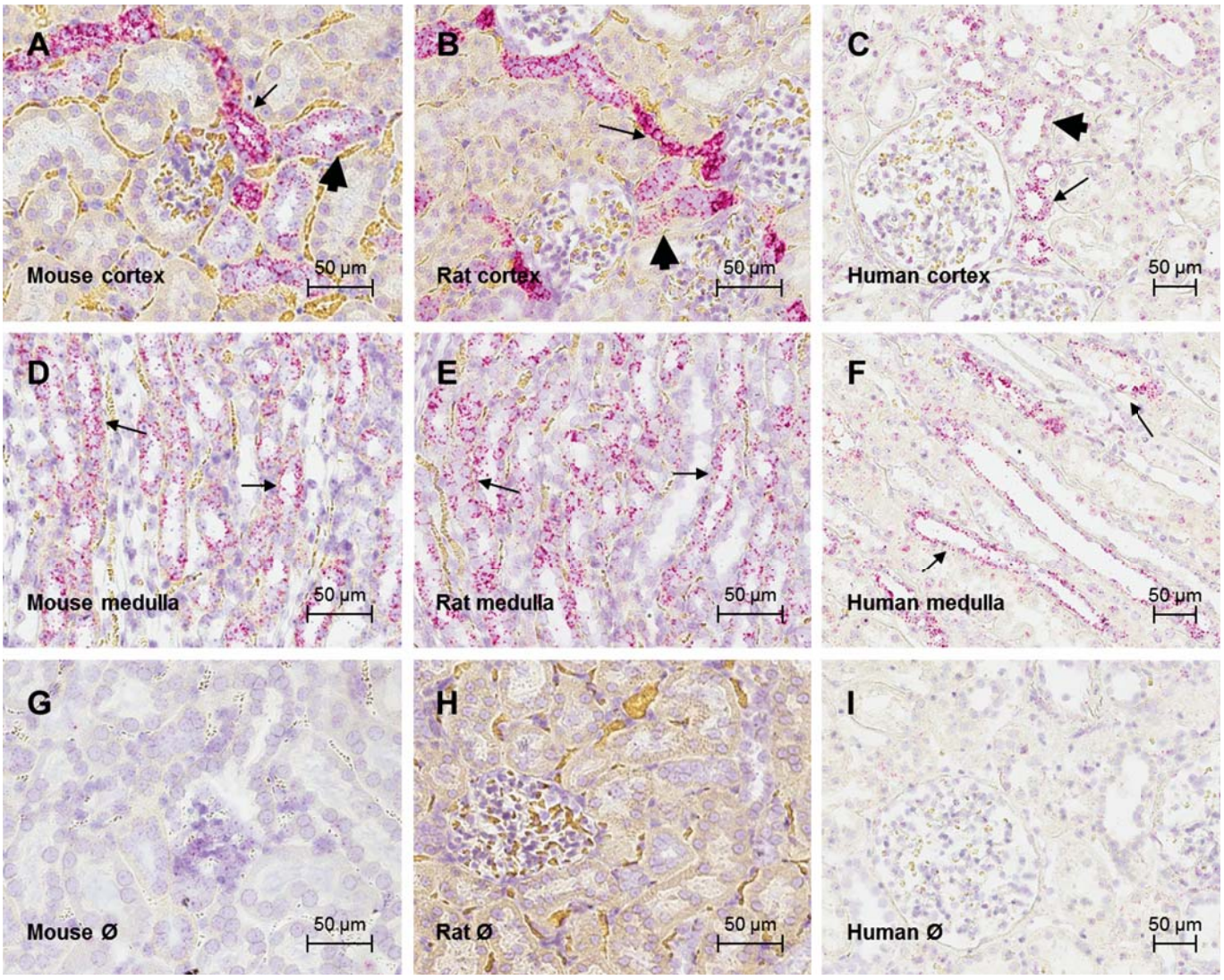
A
Mouse cortex
50 µm
B
Rat cortex
50 µm
C
Human cortex
50 µm
D
Mouse medulla
50 µm
E
Rat medulla
50 µm
F
Human medulla
50 µm
G
Mouse Ø
50 µm
H
Rat Ø
50 µm
I
Human Ø
50 µm

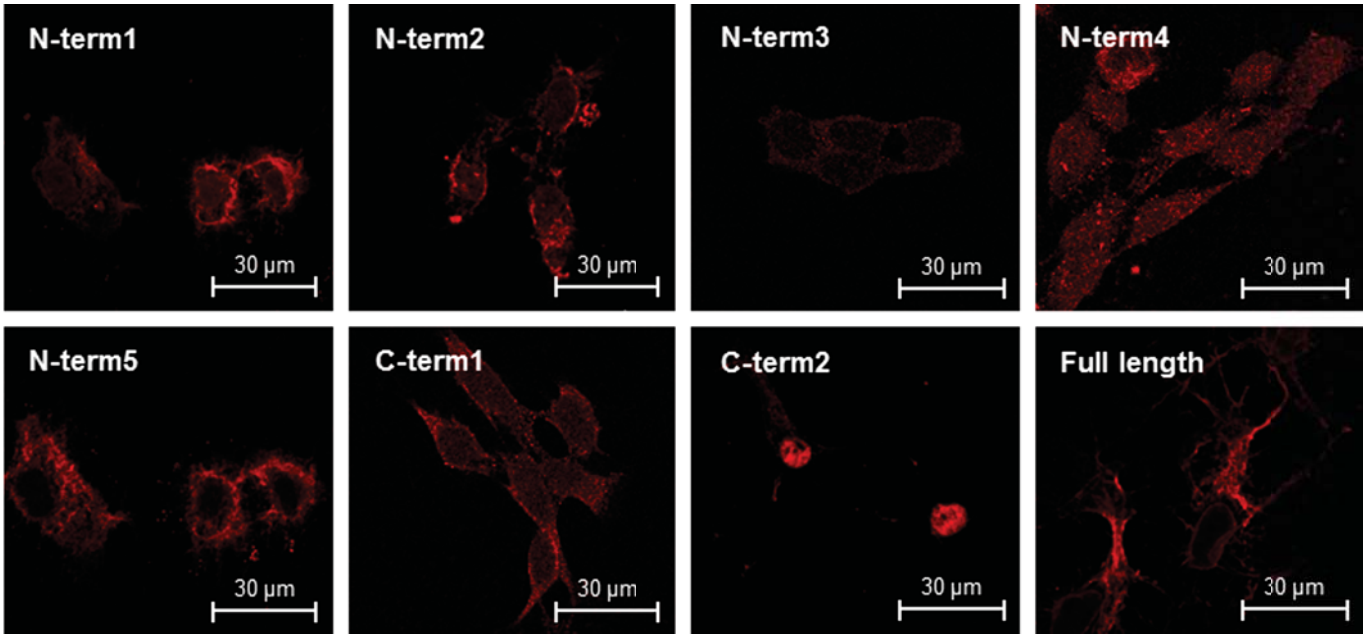
N-term1
30 µm
N-term2
30 µm
N-term3
30 µm
N-term4
30 µm
N-term5
30 µm
C-term1
30 µm
C-term2
30 µm
Full length
30 µm

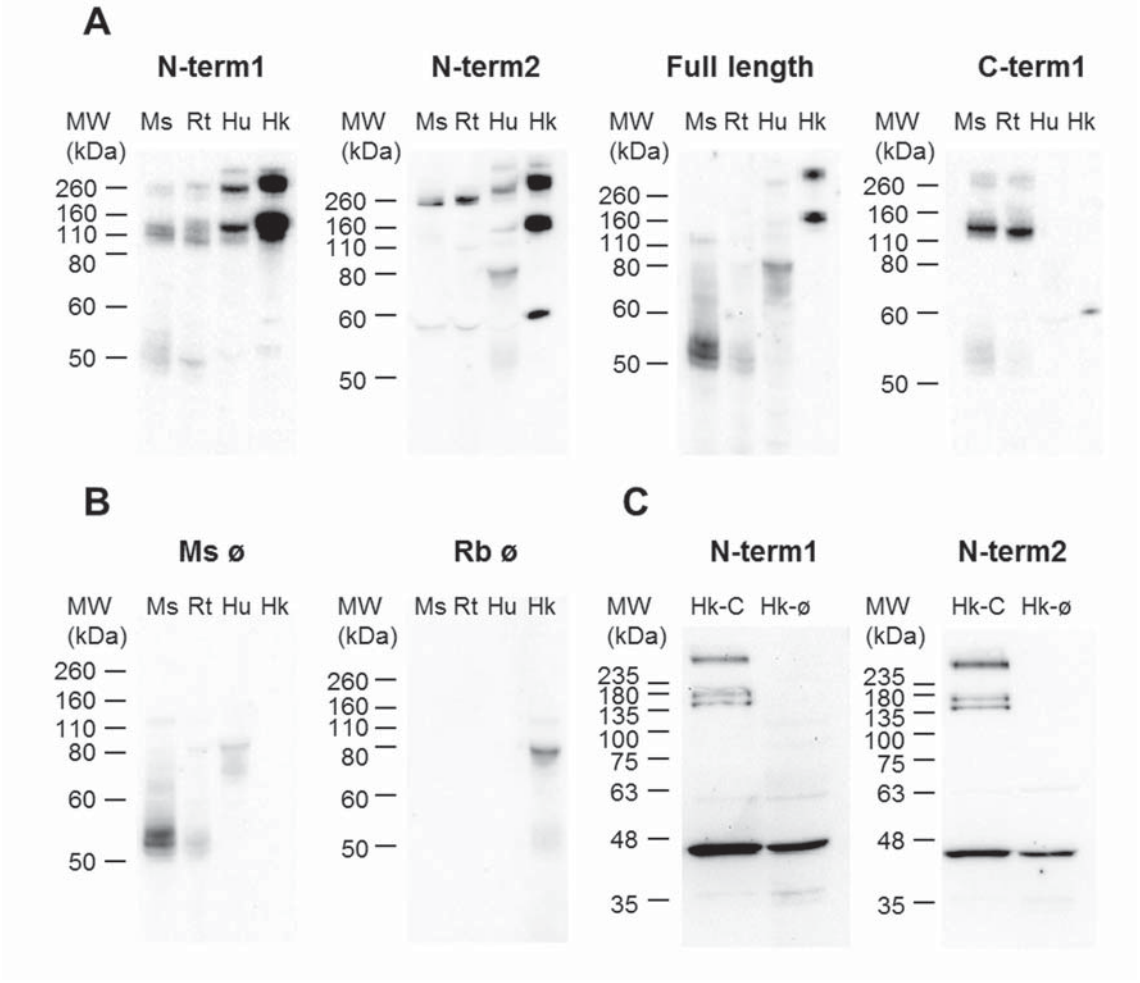
A
N-term1
N-term2
Full length
C-term1
MW (kDa)
Ms Rt Hu Hk
260
160
110
80
60
50
B
Ms ø
Rb ø
C
N-term1
N-term2
Hk-C Hk-ø
235
180
135
100
75
63
48
35

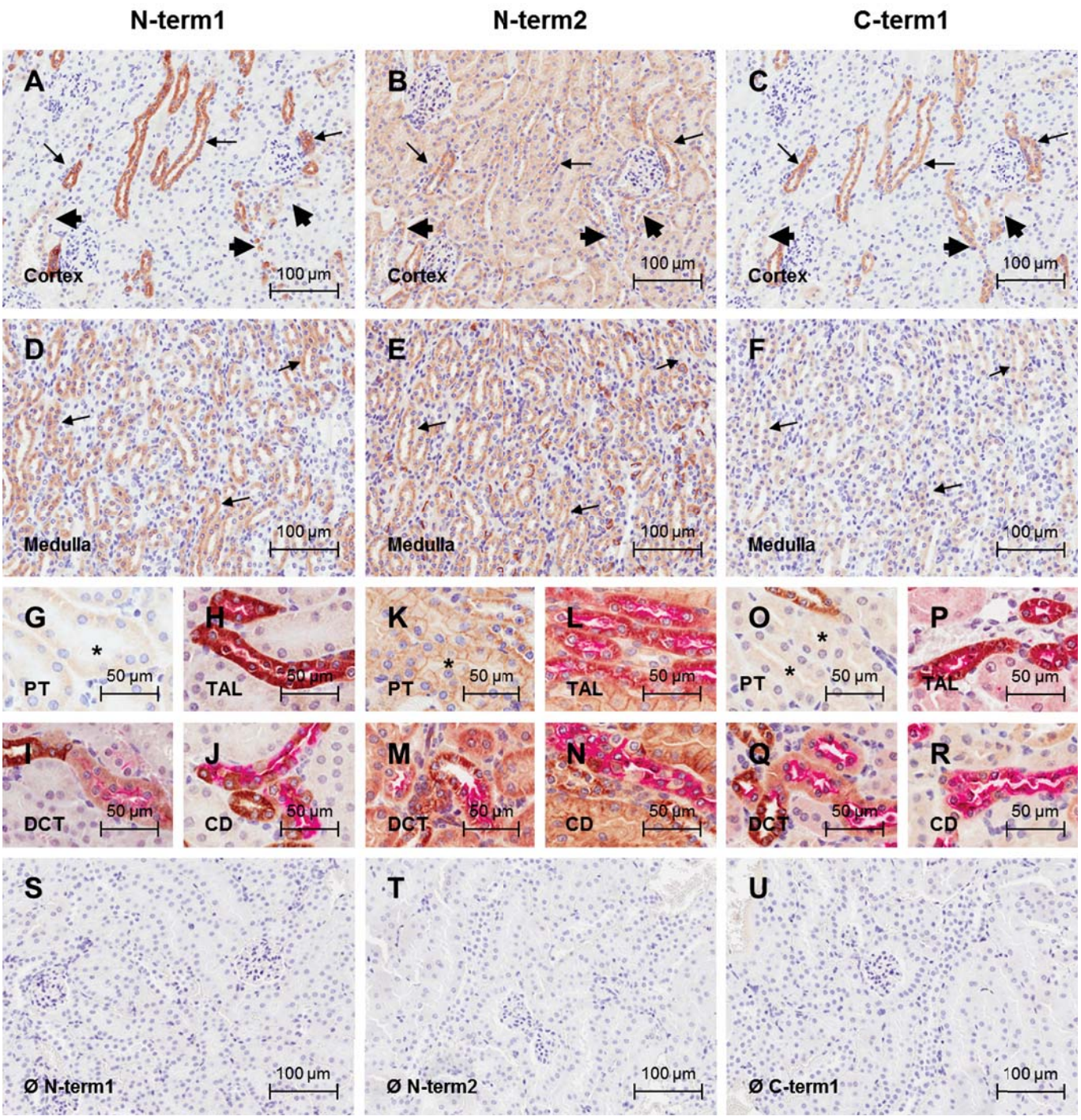
N-term1
N-term2
C-term1
A
Cortex
100 µm
B
Cortex
100 µm
C
Cortex
100 µm
D
Medulla
100 µm
E
Medulla
100 µm
F
Medulla
100 µm
G
PT
50 µm
H
TAL
50 µm
K
PT
50 µm
L
TAL
50 µm
O
PT
50 µm
P
TAL
50 µm
I
DCT
50 µm
J
CD
50 µm
M
DCT
50 µm
N
CD
50 µm
Q
DCT
50 µm
R
CD
50 µm
S
Ø N-term1
100 µm
T
Ø N-term2
100 µm
U
Ø C-term1
100 µm

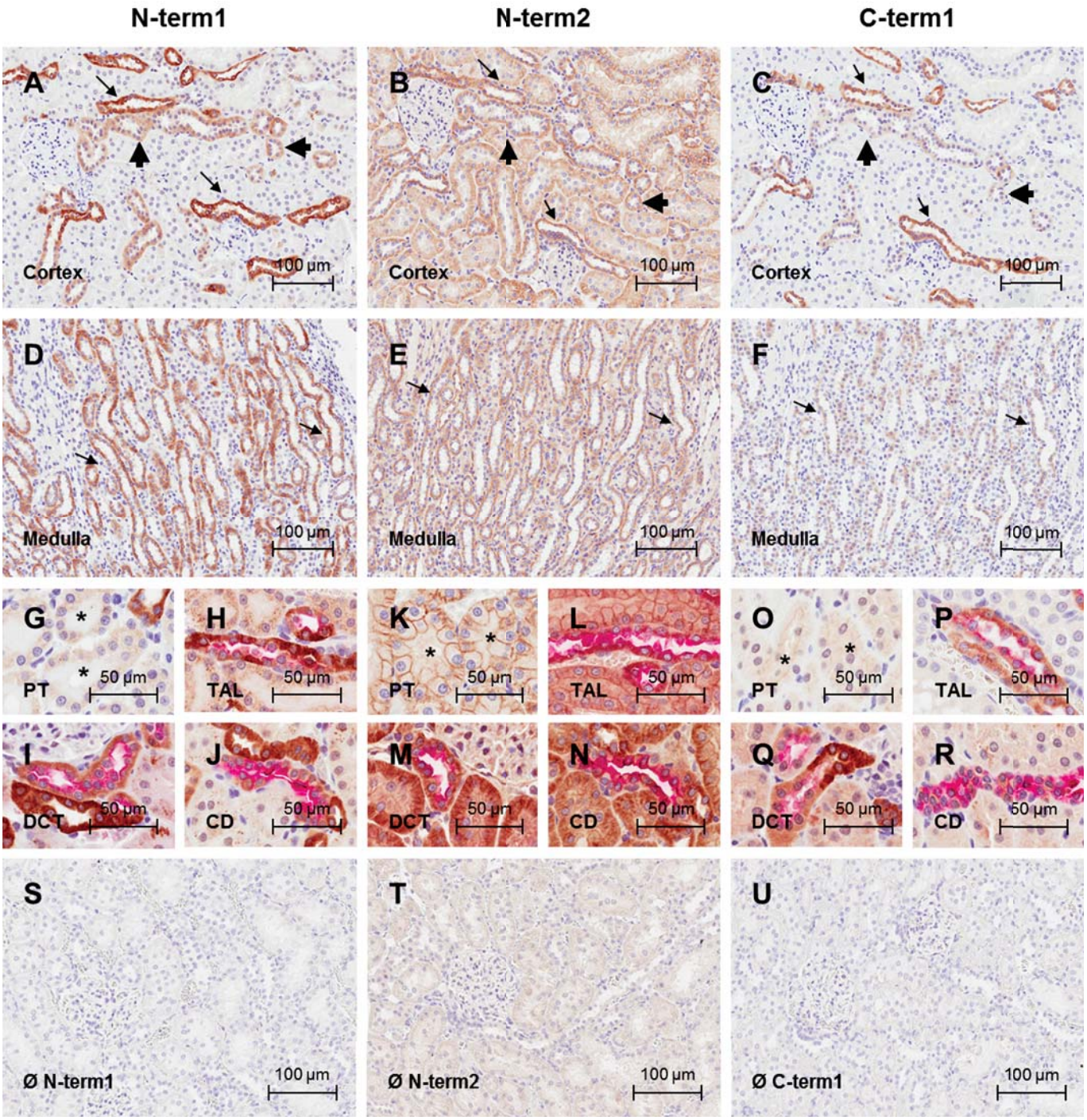
N-term1
N-term2
C-term1
A
B
C
Cortex
100 µm
D
E
F
Medulla
G
H
K
L
O
P
PT
TAL
50 µm
I
J
M
N
Q
R
DCT
CD
S
T
U
Ø N-term1
Ø N-term2
Ø C-term1

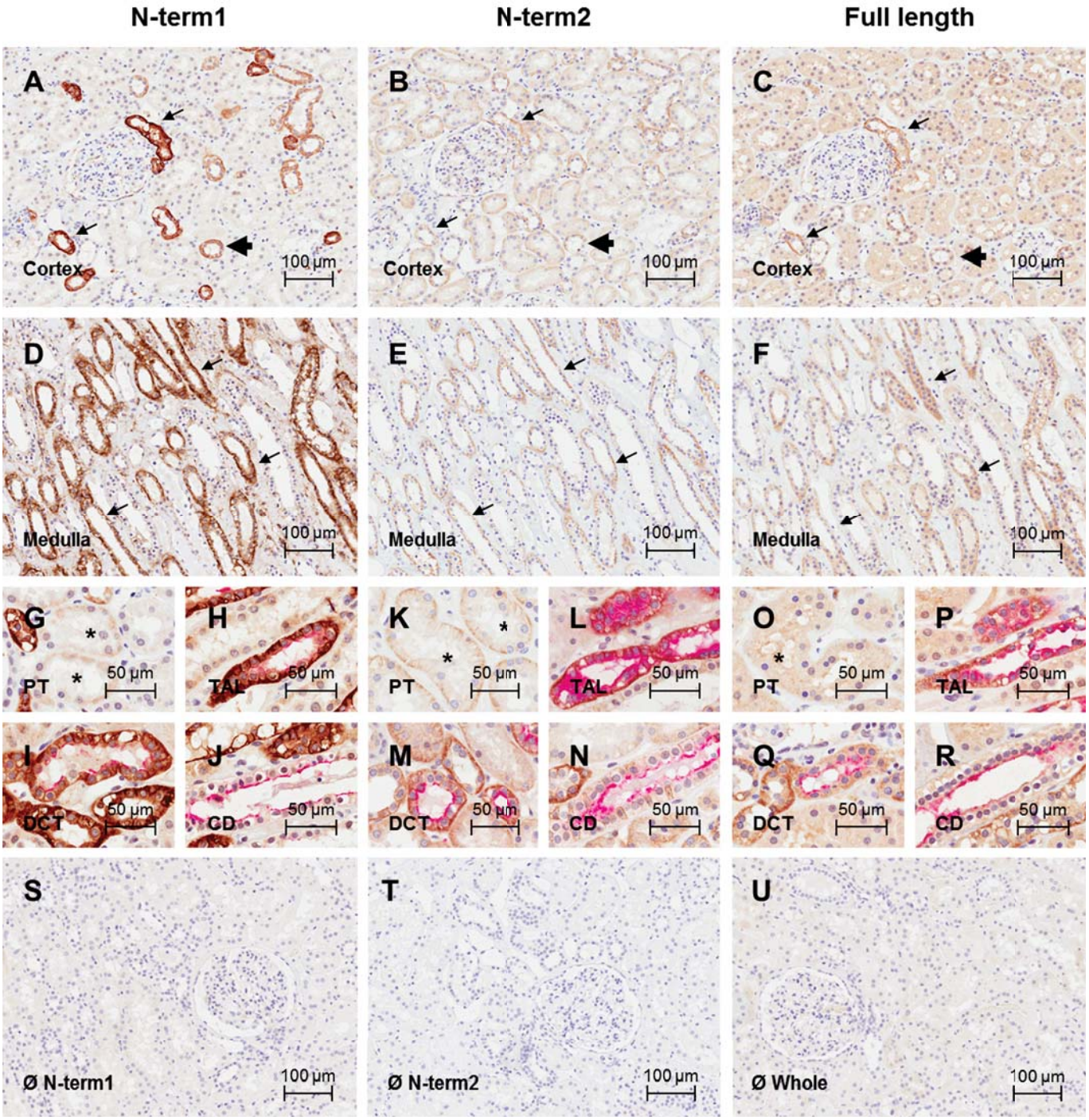
N-term1
N-term2
Full length
A
B
C
Cortex
Cortex
Cortex
100 µm
100 µm
100 µm
D
E
F
Medulla
Medulla
Medulla
100 µm
100 µm
100 µm
G
H
K
L
O
P
PT
TAL
PT
TAL
PT
TAL
50 µm
50 µm
50 µm
50 µm
50 µm
50 µm
I
J
M
N
Q
R
DCT
CD
DCT
CD
DCT
CD
50 µm
50 µm
50 µm
50 µm
50 µm
50 µm
S
T
U
Ø N-term1
Ø N-term2
Ø Whole
100 µm
100 µm
100 µm

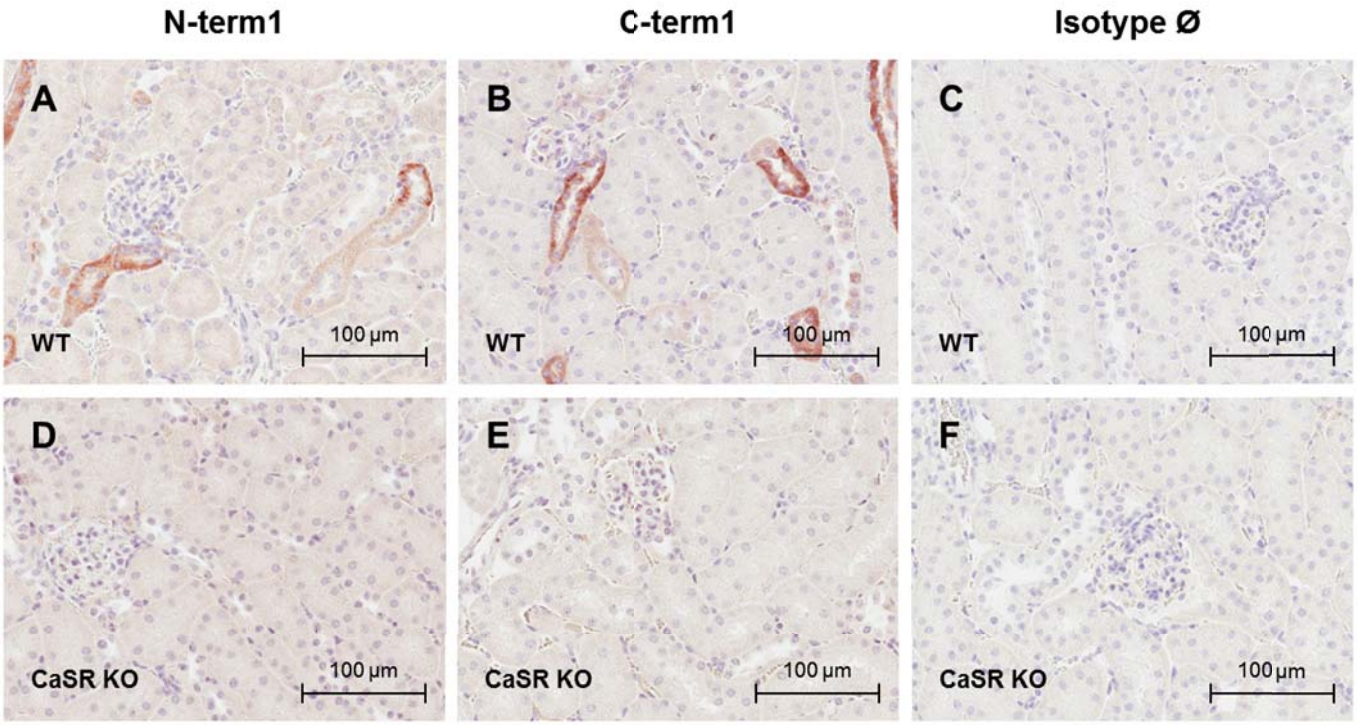
N-term1
C-term1
Isotype Ø
A
B
C
WT
WT
WT
100 µm
100 µm
100 µm
D
E
F
CaSR KO
CaSR KO
CaSR KO
100 µm
100 µm
100 µm

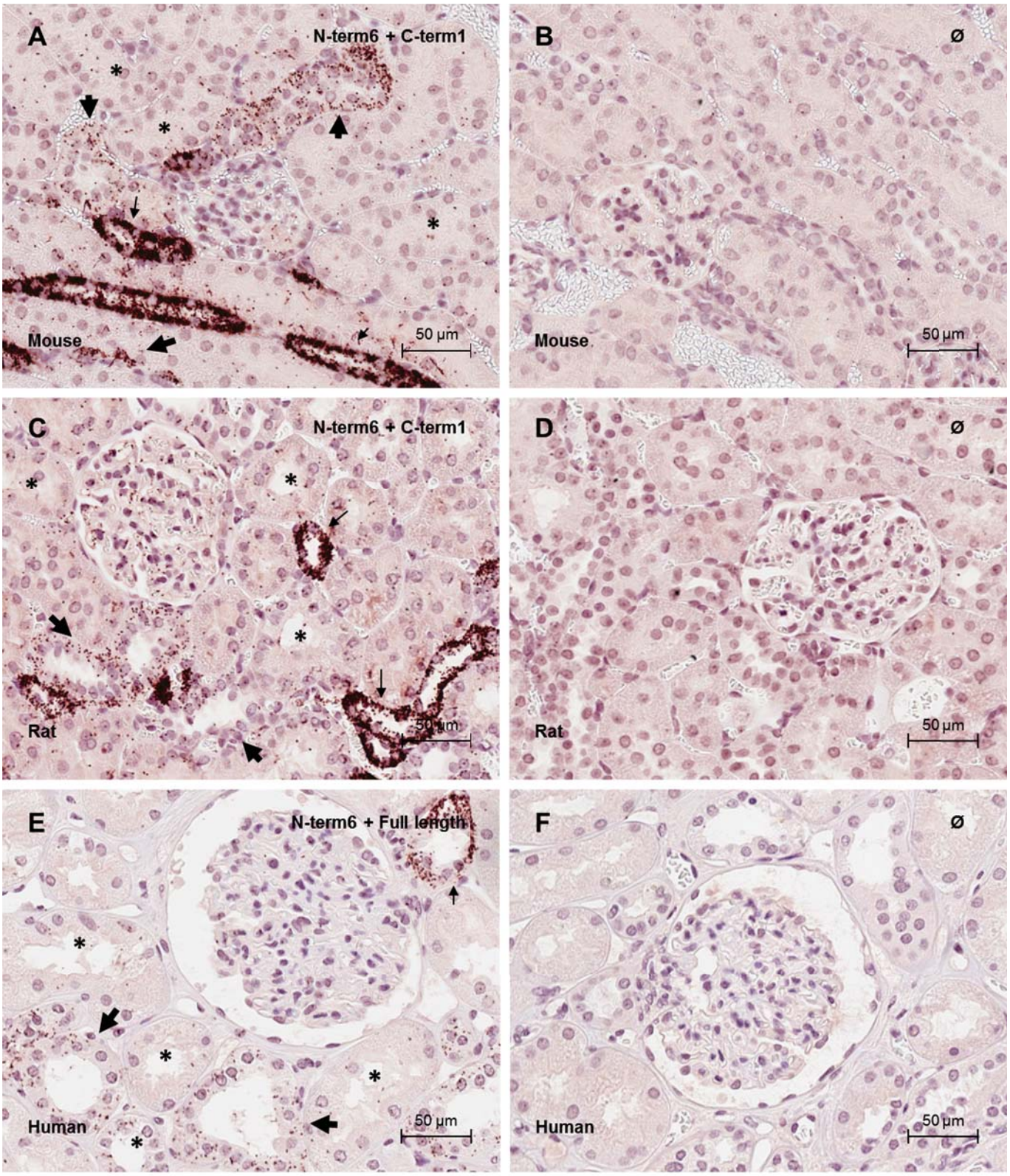
A
N-term6 + C-term1
Mouse
50 µm
B
Ø
Mouse
50 µm
C
N-term6 + C-term1
Rat
50 µm
D
Ø
Rat
50 µm
E
N-term6 + Full length
Human
50 µm
F
Ø
Human
50 µm

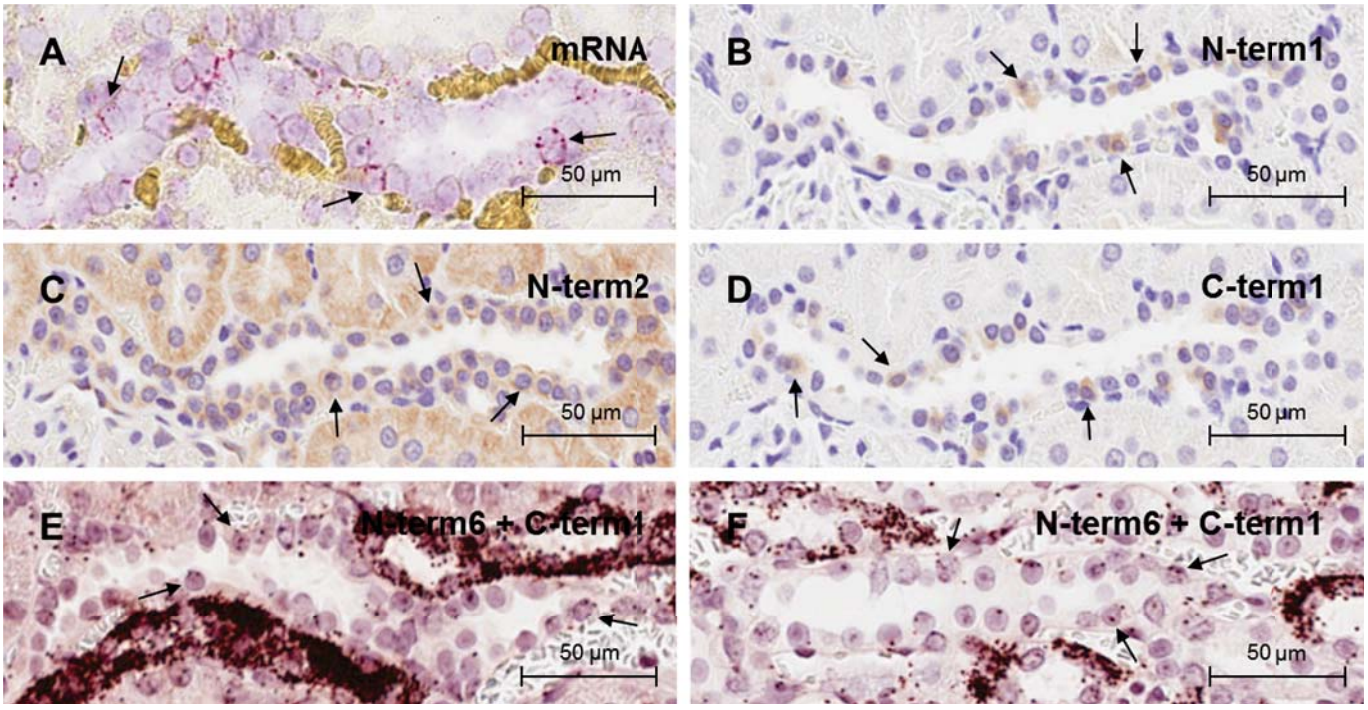
A
mRNA
50 µm
B
N-term1
50 µm
C
N-term2
50 µm
D
C-term1
50 µm
E
N-term6 + C-term1
50 µm
F
N-term6 + C-term1
50 µm

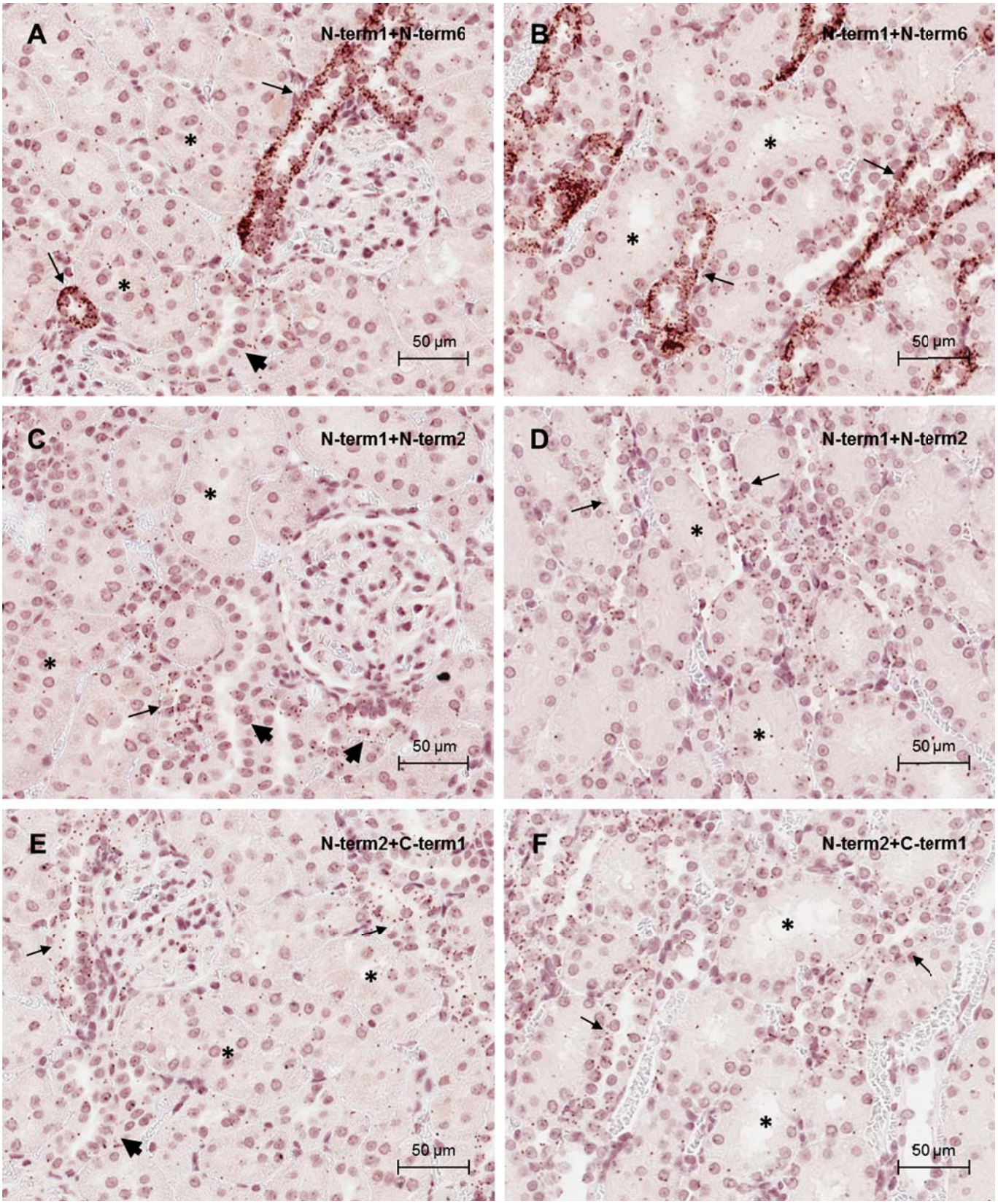
A
N-term1+N-term6
50 µm
B
N-term1+N-term6
50 µm
C
N-term1+N-term2
50 µm
D
N-term1+N-term2
50 µm
E
N-term2+C-term1
50 µm
F
N-term2+C-term1
50 µm

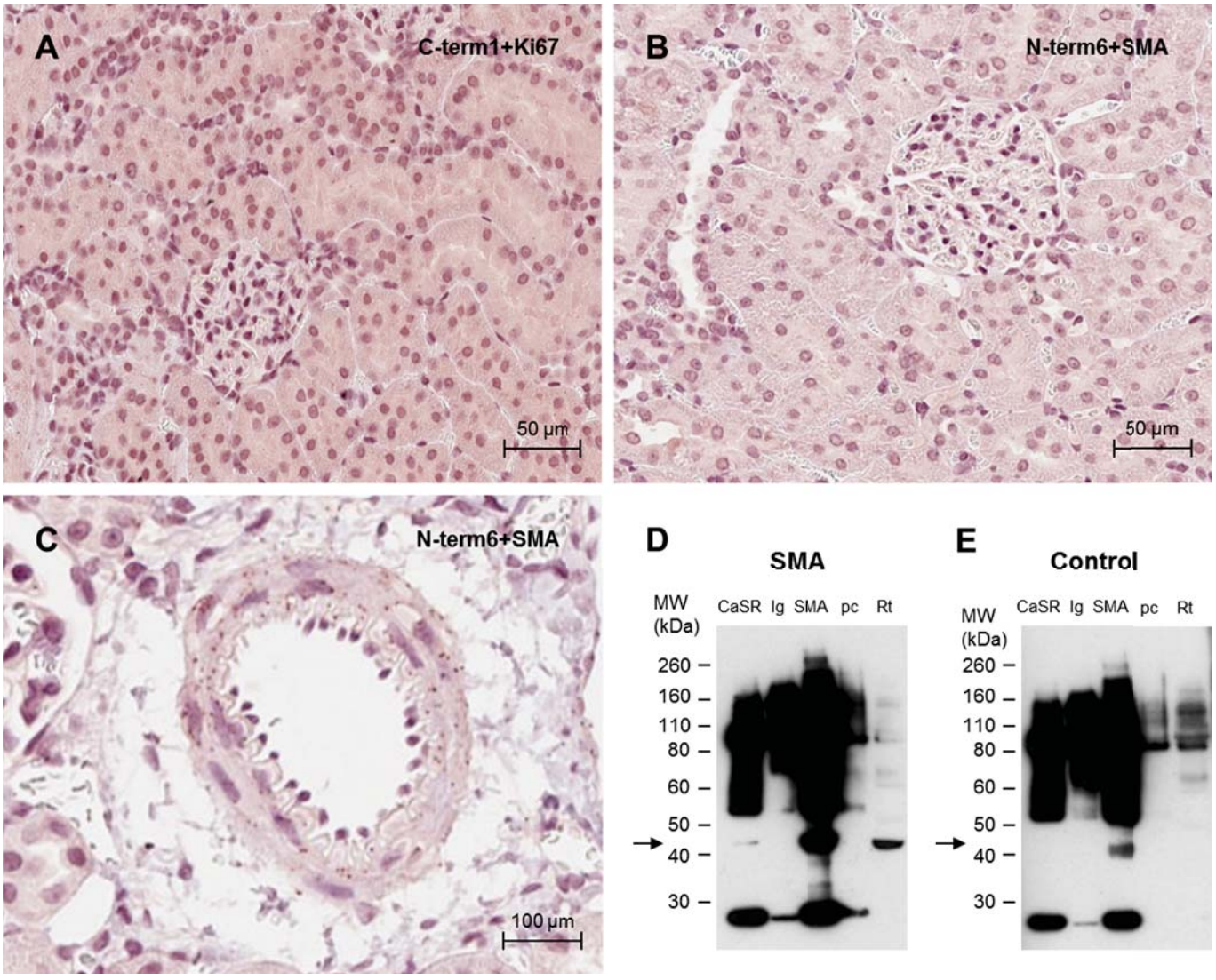
A
C-term1+Ki67
50 µm
B
N-term6+SMA
50 µm
C
N-term6+SMA
100 µm
D
SMA
MW (kDa)
CaSR Ig SMA pc Rt
260
160
110
80
60
50
40
30
E
Control
MW (kDa)
CaSR Ig SMA pc Rt
260
160
110
80
60
50
40
30

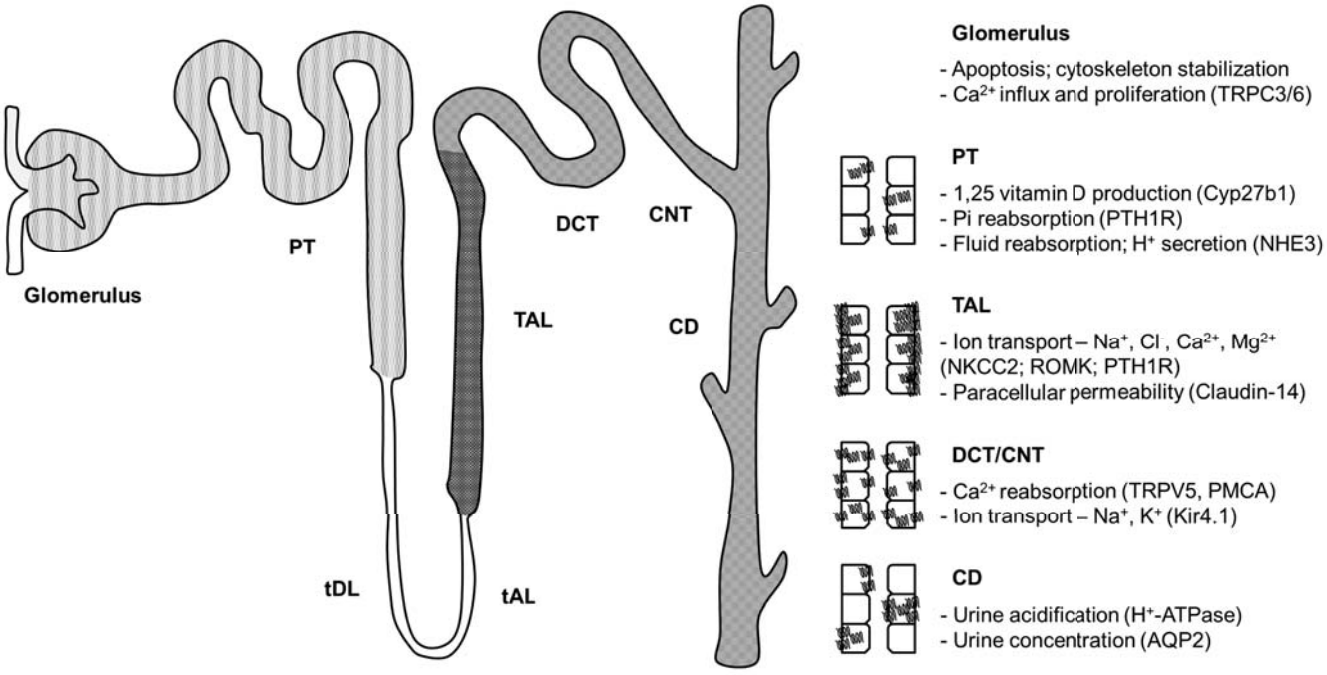
Glomerulus
PT
DCT
CNT
TAL
CD
tDL
tAL
Glomerulus
- Apoptosis; cytoskeleton stabilization
- Ca2+ influx and proliferation (TRPC3/6)
PT
- 1,25 vitamin D production (Cyp27b1)
- Pi reabsorption (PTH1R)
- Fluid reabsorption; H+ secretion (NHE3)
TAL
- Ion transport – Na+, Cl , Ca2+, Mg2+ (NKCC2; ROMK; PTH1R)
- Paracellular permeability (Claudin-14)
DCT/CNT
- Ca2+ reabsorption (TRPV5, PMCA)
- Ion transport – Na+, K+ (Kir4.1)
CD
- Urine acidification (H+-ATPase)
- Urine concentration (AQP2)